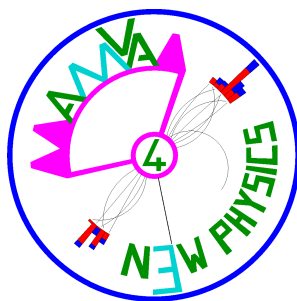




This Report is part of a project that has received funding from the **European Union's Horizon 2020 research and innovation programme** under grant agreement N°675440



AMVA4NewPhysics ITN

WORK PACKAGE 4 - DELIVERABLE 4.2

Report on a Statistical Learning method for Model-Independent searches for New Physics

December 28, 2017

Abstract

Model-Independent searches for New Physics at the Large Hadron Collider can be stated as a collective anomaly detection problem. We propose the parametric approach that uses a semi-supervised learning algorithm. It is based on a penalized likelihood and is able to jointly perform appropriate variable selection and detect possible collective anomalous behavior in data with respect to a given background sample. The proposed algorithm is tested both on synthetic and simulated data from the Large Hadron Collider.

1 Introduction

One of the main goals of the Large Hadron Collider (LHC) physics program is to probe the current theory of elementary particle physics, known as the Standard Model, and to further discover phenomena beyond that theory if they occur. The LHC accelerates protons in a 27 km ring that lead to collisions with a center of mass energy of 13 TeV each 25 ns, making it the largest and most powerful collider to date. General-purpose detectors at the LHC, namely ATLAS and CMS, have been primarily designed to measure the properties of the phenomena emerging from proton-proton collisions.

Since its conception over four decades ago the Standard Model has proven to be a successful theory, its predictions go from precise values of parameters to the existence of particles. Nonetheless, many theoretical extensions of the Standard Model aim to solve its well-known problems (e.g. the absence of a quantum description of gravity), establishing guidelines for experimental searches for phenomena beyond the Standard Model, referred to as New Physics (NP). Experimental searches for NP usually assume hypotheses associated to the existence of some theorized NP phenomena, which are to be confirmed or ruled out to a certain extent, for example, by comparing the data with the predictions that include such phenomena in a specific region of a parameter space. However, this model-dependent approach is limited in two senses: firstly, being guided by a NP model, it fails to cover a wider space of parameters where untheorized NP could appear; and secondly, it focuses on an often small set of experimental signatures which, even after combining all existing model-dependent NP searches at the LHC, leaves a broad number of signatures unexplored [1, 2]. In order to address these issues, Model-Independent, multi-signature searches have to be performed.

This work presents a novel anomaly detection method and an application to a model independent search at the LHC. The method is oriented on collective anomaly searches and employs a semi-supervised learning approach to cope with the scenario in which no physics knowledge for an anomaly is provided a priori. Special care is taken to perform proper variable selection and in the use of the two related input datasets: one that contains only Standard Model physics events and another that could additionally contain a set of anomalous events. Results for simulated synthetic data and for a dijet search at the LHC are presented as a proof of concept.

This document is organized as follows. In Section 2 we describe the physics problem and pose it in statistical terms. We then describe the method introduced by this work on section 3, followed by results of the application of the method in artificial data and in a search at the LHC using a simulated datasets that contain a NP signal, in Sections 4 and 5, respectively. Concluding remarks are presented in Section 6.

2 Description of the problem

Detectors such as ATLAS and CMS can identify and measure with precision most final-state particles produced in proton-proton collisions: photons (γ), leptons (e , μ , τ) and jets (j), including those that originate from a b quark decay, known as b -jets. One can classify each collision event according to its particle content in the final state, a so-called experimental signature, thereby allowing to separate the events in different case studies.

The goal of NP search analyses is to find evidence of the existence of new possible particles not predicted by the Standard Model. The main underlying assumption is that such new particles, if they do exist, show an anomalous behavior with respect to the known Standard Model physics. Within the Model Independent approach one relies on the prediction of the Standard Model processes, the so-called background, in general obtained by Monte Carlo (MC) simulations, to be compared with the actual experimental data that could additionally contain events coming from a NP process. For the purpose of this study, both background and experimental data were produced using the MC simulation packages MADGRAPH5 [3], PYTHIA8 [4, 5], and DELPHES [6], as described in section 5, where NP signal events are injected in the experimental data with different proportions on top of the Standard Model processes in order to assess the power and limitations of the method presented.

There have been several efforts in the CMS and ATLAS collaborations to perform Model Independent searches. In particular, there are signature-specific searches as, e.g., the ones in [7, 8]. More generally, both experimental collaborations have performed Model Independent searches for NP in a systematic way in many signatures [9, 10, 11, 12, 13], an approach denominated General Search. Automatically exploring multiple signatures entails analyses of high volumes of data and in general LHC searches have been based on a simple uni-variate analysis. This approach consists in separating data and simulated events into hundreds of independent experimental signatures; then for corresponding class of events, one-dimensional histograms for data and simulation are produced for a few kinematic variables. A simple algorithm can then be used to identify the region on each histogram where the disagreement between data and simulation is the largest. By construction, this approach is not able to capture potential anomalies that become manifest when probing the datasets in multiple variables at once, which requires a multi-variate approach, such as the one presented in this work.

From a statistical point of view, the aforementioned problem of NP search can be framed in the context of anomaly detection [14] when one searches for events, also referred to as observations, that are not consistent with an assumed model. One of the most common ways to define anomalies is to refer them as unusual events, unlikely to be observed under the assumed model. If such definition were applied to the considered problem, any signal event that has a substantial probability to be also generated by the background process would be falsely classified as non-anomalous. Consequently, the interest is put on finding groups of observations that separately

82 do not need to have anomalous properties (according to the former definition) but
 83 their common occurrence in a particular part of the data domain is unexpected.
 84 This is known as “*collective anomaly*” detection.

85 Two data samples are at hand: the background - MC data, simulated according to
 86 the Standard Model, and the experimental sample, possibly also including observa-
 87 tions from the unknown signal. Since there is only a partial knowledge of processes
 88 generating the datasets, the anomaly detection problem emerges as semi-supervised
 89 learning approach. Simulated data are labelled as drawn from the background,
 90 while no direct information about the generating process of the experimental data,
 91 which we then refer to as unlabelled.

92 Hence, we shall operate in an unsupervised manner and later strengthen the
 93 classification power based on the accessible labels of the background observations.
 94 The starting point for our approach is found in Vatanen et al. [15] and Kuusela et al.
 95 [16] and is described in the following section.

96 3 Methods

97 3.1 Modeling data by mixture models

98 Let $X = (\mathbf{x}_1, \dots, \mathbf{x}_n)'$ be the sample of the MC background data, where for $i = 1, \dots, n$,
 99 $\mathbf{x}_i = (x_{i1}, \dots, x_{ip}, \dots, x_{iP})'$ are i.i.d. P -dimensional observations with unknown prob-
 100 ability density function f_B . Also, denote by $Y = (\mathbf{y}_1, \dots, \mathbf{y}_m)'$ the experimental data,
 101 where for $i = 1, \dots, m$, $\mathbf{y}_i = (y_{i1}, \dots, y_{ip}, \dots, y_{iP})'$ are i.i.d. observations from the un-
 102 known probability density function f_{SB} . It is natural to assume for f_{SB} a mixture of
 103 the two components:

$$f_{SB}(\mathbf{y}) = (1 - \lambda)f_B(\mathbf{y}) + \lambda f_S(\mathbf{y}) \quad (1)$$

104 where f_B and f_S are the background and signal distributions respectively. Parameter
 105 $\lambda \in [0, 1]$ represents the proportion of the signal events in the whole data Y .

106 The models for the background and signal should be arbitrarily flexible so that
 107 even complex processes could be well represented. For this reason we assume that
 108 both f_S and f_B are mixtures. In particular we consider finite mixtures of Gaussian
 109 distributions as they are capable of approximating well every distribution. The
 110 Gaussian mixtures suit particularly well as they have been proven to serve well for
 111 density estimation and for classification purposes [17]. Hence, let us specify the two
 112 models for the background and signal respectively as

$$f_B(\mathbf{y}) = \sum_{k=1}^K \pi_k \phi(\mathbf{y} | \boldsymbol{\mu}_k, \Sigma_k) \quad \text{and} \quad f_S(\mathbf{y}) = \sum_{q=1}^Q \pi_q \phi(\mathbf{y} | \boldsymbol{\mu}_q, \Sigma_q) \quad (2)$$

where K and Q are the numbers of Gaussian components in the mixtures, π_k and
 π_q for $k = 1, \dots, K$ and $q = 1, \dots, Q$ are the mixing proportions (with the constraints

$\sum_{k=1}^K \pi_k = 1$ and $\sum_{q=1}^Q \pi_q = 1$) and $\phi(\mathbf{y}|\boldsymbol{\mu}, \Sigma) = \frac{1}{(2\pi)^{\frac{p}{2}} |\Sigma|^{\frac{1}{2}}} \exp\left(-\frac{1}{2}(\mathbf{y} - \boldsymbol{\mu})' \Sigma^{-1} (\mathbf{y} - \boldsymbol{\mu})\right)$

denotes the P -variate Gaussian density with mean vector $\boldsymbol{\mu}$ and covariance matrix Σ . Consequently, the model for the experimental data Y is also the Gaussian mixture

$$\begin{aligned} f_{SB}(\mathbf{y}) &= (1 - \lambda) \sum_{k=1}^K \pi_k \phi(\mathbf{y}|\boldsymbol{\mu}_k, \Sigma_k) + \lambda \sum_{q=1}^Q \pi_q \phi(\mathbf{y}|\boldsymbol{\mu}_q, \Sigma_q) \\ &= \sum_{l=1}^{K+Q} \tilde{\pi}_l \phi(\mathbf{y}|\boldsymbol{\mu}_l, \Sigma_l), \end{aligned}$$

113 where $\tilde{\pi}_k$ are mixture proportions accounting for the λ and naturally $\sum_{l=1}^{K+Q} \tilde{\pi}_l = 1$
114 holds.

Parameters of a mixture model are usually estimated via maximum likelihood. Consider, for the sake of simplicity, the estimation of the parameters involved in f_B (equation 2). Conditionally to the observation of the X data, the log-likelihood is defined as:

$$\log L_p(\theta) = \sum_{i=1}^n \log \left[\sum_{k=1}^K \pi_k \phi_k(\mathbf{x}_i | \boldsymbol{\mu}_k, \Sigma_k) \right],$$

115 where $\theta = (\pi_1, \dots, \pi_K, \boldsymbol{\mu}_1, \dots, \boldsymbol{\mu}_K, \Sigma_1, \dots, \Sigma_K)$ are model parameters. In literature the
116 mixture components are often related to data clusters [17] and the background es-
117 timation could be referred as model-based clustering. Since the optimization of the
118 likelihood has no explicit solution, numeric methods have to be used. Here we em-
119 ploy the Expectation-Maximization (EM) algorithm [18]. The method relies on an
120 iterative two-steps loop. The first step is to compute the expectation for each ob-
121 servation to belong to a given component and it is computed based on the current
122 parameter values. Subsequently, conditioning on the expectations (posterior proba-
123 bilities of cluster membership) the parameter estimates are updated as the result of
124 maximum likelihood optimization.

125 The algorithm is described by the following formulas:

- 126 • Expectation step - given current values of the estimates the probability of the
127 observation \mathbf{x}_j belonging to the l^{th} cluster (component) is:

$$\tau_{il}^{(r)} = \frac{\pi_l^{(r)} \phi(\mathbf{x}_i | \boldsymbol{\mu}_l^{(r)}, \Sigma_l^{(r)})}{\sum_{k=1}^K \pi_k^{(r)} \phi(\mathbf{x}_i | \boldsymbol{\mu}_k^{(r)}, \Sigma_k^{(r)})}. \quad (3)$$

- 128 • Maximization step - given posterior probabilities τ_{il} update the current pa-
129 rameter estimates

130 – Component proportions for $k = 1, \dots, K$

$$\hat{\pi}_k^{(r+1)} = \frac{1}{n} \sum_{i=1}^n \tau_{ik}^{(r)}. \quad (4)$$

131 – Component mean parameters for $k = 1, \dots, K$ and $p = 1, \dots, P$

$$\hat{\mu}_{kp}^{(r+1)} = \frac{\sum_{i=1}^n \tau_{ik}^{(r)} x_{ip}}{\sum_{i=1}^n \tau_{ik}^{(r)}} \quad (5)$$

132 – Component covariance matrices

$$\hat{\Sigma}_k = \frac{\sum_{i=1}^n \tau_{ik}^{(r)} * (\mathbf{x}_i - \hat{\boldsymbol{\mu}}_k^{(r)})(\mathbf{x}_i - \hat{\boldsymbol{\mu}}_k^{(r)})'}{\sum_{i=1}^n \tau_{ik}^{(r)}}. \quad (6)$$

133 The upper index (r) indicates the subsequent iterations of the algorithm. Each iteration
 134 of the EM algorithm has been proven to increase the model likelihood. The loop
 135 iterations are performed until the estimates converge, i.e. changes of the likelihood
 136 between the subsequent iteration are arbitrarily small.

137 In order to obtain a solution for the semi-supervised problem of anomaly detec-
 138 tion we stem from the *fixed-background* model introduced in Vatanen et al. [15] and
 139 Kuusela et al. [16]. The main idea underlying those works is to estimate the model
 140 parameters in a 2-step procedure: first based on the background data X the model
 141 $f_B(\mathbf{x})$ is fitted. In the second step for the experimental data Y , the model parameters
 142 are estimated by keeping the background parameters fixed (component proportions
 143 are adjusted according to λ value).

144 3.2 Dimensionality reduction methods in mixture models

145 The fixed-background model is built upon a natural idea and makes a logical use
 146 of the two datasets. However, as pointed out by the authors, for high dimensional
 147 spaces the model suffers from the curse of dimensionality. This affects both the
 148 ability to find possible signal components and, possibly, the algorithm convergence.
 149 For data of dimension P , the number of free parameters to be estimated is large -
 150 for each covariance matrix $\frac{P(P+1)}{2}$ parameters, KP for mean vectors and $K - 1$ for
 151 mixture proportions, giving a total amount of $\frac{K(P+1)(P+2)}{2} - 1$ free parameters.

152 It follows the need of reducing the dimensionality of the parameter space. Vata-
 153 nen et al. [15] perform principal component analysis of the original space and run
 154 the anomaly detection algorithm in the reduced space spread on the first few com-
 155 ponents. However, there is absolutely no guarantee that the first few selected prin-
 156 cipal components exhibit any deviation of the signal distribution versus the back-
 157 ground, in presence of an anomalous component. Alternatively, in the context of

158 anomaly detection,[19] perform variable selection based on some heuristics, i.e.
 159 criteria related to the divergence between the marginal distributions of the back-
 160 ground and experimental data. The proceeding estimation of parameters is per-
 161 formed subsequently as if the two tasks were independent. In the unsupervised
 162 context of model-based clustering, several approaches have been introduced to re-
 163 duce the number of parameters. In Banfield and Raftery [20] parsimonious mixtures
 164 of Gaussian distributions are proposed. The specific constraints on the component
 165 covariance matrices are set so that the number of free parameters is greatly reduced
 166 (for example by using component-specific diagonal covariance matrices). Based on
 167 that idea the model-based clustering framework was proposed by Celeux and Go-
 168 vaert [21] . In a similar manner Bouveyron et al. [22] proposed another family of
 169 Gaussian mixture models with other type of constraints on component covariance
 170 matrices.

An alternative approach to reduce the number of parameters to be estimated is to jointly perform parameter estimation and variable selection. In the field of statistical regression such approach is common [23, 24] and it makes use of an estimates-based penalty function. In this setting, the most relevant example is the LASSO [25], where the number of model free parameters is decreased by introducing a penalization of the optimization function, causing parameters shrinkage to a fixed value (possibly to 0). In general, instead of the log-likelihood optimization, the aim is to maximize the penalized log-likelihood expression:

$$\log L_p(\theta) = \log L(\theta) - \gamma p(\theta).$$

171 were γ is a regularization parameter and $p(\theta)$ is a penalty function of the model pa-
 172 rameters θ . The regularization parameter γ serves as a balance between bias of the
 173 estimates and small penalty value. Penalty introduces bias with respect to the stan-
 174 dard maximum likelihood solution but on the other hand, it decreases the variance
 175 of the estimates that results in better model performance in terms of mean square
 176 error.

177 The origin of the penalized approach for mixture models should be found in Pan
 178 and Shen [26]. The authors proposed a penalized log-likelihood that automatically
 179 performs variable selection. For the standardized data, it is proposed to shrink
 180 component mean parameters to 0 under assumption that the component covariance
 181 matrices are equal to identity. The authors considered the following form of the
 182 penalized log-likelihood

$$\log L_p(\theta) = \sum_{i=1}^n \log \left[\sum_{k=1}^K \pi_k \phi_k(\mathbf{x}_i | \boldsymbol{\mu}_k, \Sigma_k) \right] - \gamma \sum_{k=1}^K \sum_{p=1}^P |\mu_{kp}|. \quad (7)$$

183 The Maximum Penalized Log-likelihood Estimates (MPLE) are found using a modi-
 184 fied EM algorithm (for details we refer to the source article). Shrinkage of the mean
 185 parameters to 0 is not only causing the regularization but serves for feature selec-
 186 tion, as described in subsection 3.3.3.

187 Xie [27] relaxes the assumption of the identity covariance matrices to the component-
 188 specific diagonal covariance matrices. A second penalty term is introduced, which
 189 encourages diagonal elements of the covariance matrices to be equal to 1 while it
 190 also leads to variable selection in similar manner. In parallel Zhou et al. [28] con-
 191 sider another penalty as a function of the covariance matrices. Specifically, it is a
 192 function of the elements of the component-specific covariance matrix inverses, that
 193 is applied to enable the needed regularization.

In contrast to Pan and Shen [26] where a l_1 penalty of the mean parameters is considered (equation 7) Xie et al. [29] introduces a l_2 penalty on the means that simultaneously shrinks a whole vector of parameters for particular variables. They consider the following penalized log-likelihood formula:

$$\log L_p(\theta) = \sum_{i=1}^n \log \left[\sum_{k=1}^K \pi_k \phi_k(\mathbf{x}_i | \boldsymbol{\mu}_k, \Sigma_k) \right] - \gamma \sum_{p=1}^P \|\boldsymbol{\mu}_{\cdot p}\|,$$

194 where $\|\boldsymbol{\mu}_{\cdot p}\| = \sqrt{\sum_{k=1}^K \mu_{kp}}$ for $p = 1, \dots, P$. The l_1 penalty causes shrinkage of the mean
 195 parameters individually and variable selection is performed if and only if for some
 196 $p = 1, \dots, P$ and all $k = 1, \dots, K$ $\mu_{kp} = 0$. In order to obtain the effective shrinkage to
 197 0 for a given variable of all the component-specific mean parameters, the grouped
 198 shrinkage is more suitable, i.e. it is the case for the grouped LASSO [30]. For the
 199 grouped penalty it is more likely that the true uninformative variables are removed
 200 and less bias is introduced to the estimates of the informative variable-dependent
 201 parameters.

202 In the semi-supervised context, the idea for a penalized algorithm for dimension
 203 reduction was introduced in Pan et al. [31]. The authors consider the mixture of
 204 Gaussian models and propose a shrinkage method for parameters to obtain sparse
 205 solutions in a related manner to the LASSO. However in Pan et al. [31], a slightly
 206 different anomaly detection problem is considered. In their case a single partially
 207 labeled dataset is considered and it is assumed that each Gaussian component of
 208 the model corresponds to a single label. However, for the considered problem of
 209 this paper, an interplay of the two datasets at hand is studied. The datasets have
 210 different origin and in general could vary in size. First, if the two sets were merged,
 211 the possible signal fraction in the produced data is decreased resulting in poorer
 212 anomaly detection power. The second discrepancy with the considered problem in
 213 this paper is that the background observations should not be modeled by a single
 214 Gaussian component as the true distribution of the physical processes is much more
 215 complex.

216 3.3 A penalized approach in mixture models

217 3.3.1 Penalization of the background

218 In the following we consider a comprehensive approach to jointly estimate the pa-
219 rameters and reduce the data dimensionality P by borrowing and extending the
220 fixed-background model idea [15, 16] and the parameter penalization approach de-
221 scribed in [31].

222 Since the fixed-background model is a two-step procedure, firstly requiring es-
223 timation of the background distribution in an unsupervised manner, variable selec-
224 tion based on penalization has to be primarily defined in the model-based clustering
225 setting. In the following, we extend the approach of Xie [27] by relaxing constraints
226 on the component-specific covariance matrices to be arbitrary. The proposed pro-
227 cedure makes use of two penalties as the mean for variable selection: the first is
228 a function of the component mean parameters and the second a function of the
229 component-specific covariance matrix eigenvalues. In the following the method is
230 referred as Mean And Eigenvalue Shrinkage algorithm (MAES).

The first penalty of the MAES algorithm (a function of components mean vec-
tors) borrows the idea of the grouped shrinkage presented in Xie et al. [29]. How-
ever, for the problem at hand the algorithm should be sensitive to precise estimation
of infrequent component parameters. According to Bühlmann and Van De Geer [32]
if the true proportions of the components differ substantially, penalty should be a
function of appropriately weighted parameters. It aims to balance an influence of
unequal components proportions, so that all the mean parameters are encouraged
to be shrunk uniformly, not mostly the one corresponding to the components with
the smallest proportions. The penalty is then formulated as follows:

$$p_1(\theta) = \sum_{p=1}^P \sqrt{\sum_{k=1}^K \pi_k \mu_{kp}^2}$$

231 where proportions π_k serve as the weights.

232 The second penalty of the MAES algorithm depends on the covariance matri-
233 ces of the components. It relies on eigenvalue decomposition of each component
234 covariance matrix and the idea is to perform a shrinkage of the smallest eigenval-
235 ues to 0. The aim is to obtain a low rank approximation of the clusters covariance
236 matrices, that should be especially effective if clusters lie in the lower dimensional
237 sub-spaces. In fact, shrinkage of parameters defining the component covariance
238 matrices, may result in non-positive-definite matrices which entails impossibility
239 of the likelihood computation. Alternatively, it is possible to formulate a gener-
240 alized Gaussian distribution by using a pseudo-determinant and a generalized in-
241 verse matrix. We considered this approach but we found that the optimization of
242 such a generalized penalized log-likelihood using the EM algorithm was unstable as
243 it often converged to the meaningless local maxima, the likelihood steps were not

244 monotone and the algorithm often locked itself in loops (back and forth changes of
 245 the parameter values between the subsequent iterations). For this reason no further
 246 results of this approach are shown.

247 In order to circumvent these problems we propose to shrink the eigenvalues to
 248 a component-specific small positive value ϵ_k . In this way, the expected regulariza-
 249 tion is performed and the likelihood can be written explicitly. Additionally, such a
 250 shrinkage prevents the EM algorithm from running into singularities of the likeli-
 251 hood if the smallest eigenvalue for some component covariance matrix tends to 0.
 252 As pointed out in [15, 16], this is a frequent issue of the EM algorithm employment.

253 If the L_k smallest eigenvalues for the k^{th} component are shrunk to ϵ_k then the
 254 number of free parameters is decreased by $\sum_{k=1}^K (L_k - 1) + \frac{(L_k - 1) * L_k}{2} = \sum_{k=1}^K \frac{(L_k - 1) * (L_k + 2)}{2}$.
 255 The first term results from equality of L_k eigenvalues, the second from the arbitrari-
 256 ness of choice of the eigenvectors associated to the smallest and equal eigenvalues
 257 (the last eigenvectors are arbitrarily chosen to fill up the orthogonal bases of the
 258 other eigenvectors associated to the larger eigenvalues).

In order to obtain a component-specific eigenvalue shrinkage, the eigenvalue decomposition for each component covariance matrix is performed:

$$\Sigma_k = Q_k D_k Q_k'$$

where D_k is a diagonal matrix of eigenvalues and Q_k matrix containing orthonormal eigenvectors q_{kp} . Let us represent by δ_{kp} the p^{th} largest eigenvalue of the matrix Σ_k . Consequently, the penalty is formulated as:

$$p_2(\theta) = \sum_{k=1}^K \sum_{p=1}^P \max(\delta_{kp}, \epsilon_k).$$

259 In contrast to the p_1 penalty, for p_2 penalty it is not necessary (although possible) to
 260 use weights in the penalty function. In practice the components covariance matrices
 261 estimation is more robust to a presence of the unbalanced clusters than the one of
 262 the components mean.

263 Selection of ϵ_k is performed based on the asymptotic distribution of the eigen-
 264 values [33]. Assuming that the L smallest eigenvalues of the population covari-
 265 ance matrix is equal to δ_{const} , the asymptotic distribution of the L smallest un-
 266 sorted eigenvalues δ_l of the sample covariance matrix is normal with the mean
 267 δ_{const} and variance $\frac{2\delta_{const}^2}{nL}$. Hence the estimate $\hat{\epsilon}_k$ is an unbiased estimator of δ_{const}
 268 if $\hat{\epsilon}_k = \frac{1}{n} \sum_{p=P-L+1}^P \delta_{kp}$ that is the mean of L smallest eigenvalues.

The parameter L_k is selected based on a sequential test with an adjustment for the significance level α . The sequential test uses partially the same data and a Bonferroni-like correction [34] is applied so that the type 1 error does not increase for the multiple testing paradigm. First, it is tested if all the eigenvalues of the k^{th} component covariance matrix are equal ($L_k = P$) against the general alternative. Let

$\bar{\delta}_k$ be the mean of all the eigenvalues of the sample covariance matrix for the k^{th} component. The rejection regions for the tested hypothesis are determined as

$$\frac{\hat{\delta}_{k1}}{\bar{\delta}_k} > 1 - \sqrt{\frac{2}{n}} * z_{\frac{\alpha}{2}} \quad \vee \quad \frac{\hat{\delta}_{kP}}{\bar{\delta}_k} < 1 + \sqrt{\frac{2}{n}} * z_{\frac{\alpha}{2}}$$

where $z_{\frac{\alpha}{2}}$ is the $\frac{\alpha}{2}$ quantile of the normal random variable. In summary, the null hypothesis is rejected if the ratio between the largest eigenvalue to the mean of eigenvalues is too large or the ratio between the smallest eigenvalue to the mean is too low. If there is no reason to reject the null then $L_k = P$, otherwise a sequential test is performed if the $P - 1$ smallest eigenvalues are equal. For this aim the largest eigenvalue estimate is discarded from the considered set, mean value $\bar{\delta}_k$ recomputed and the new rejection region determined

$$\frac{\hat{\delta}_{kh}}{\bar{\delta}_k} > 1 - \sqrt{\frac{2}{n}} * z_{\frac{\alpha}{2h}} \quad \vee \quad \frac{\hat{\delta}_{kP}}{\bar{\delta}_k} < 1 + \sqrt{\frac{2}{n}} * z_{\frac{\alpha}{2h}}$$

269 where h numerates upon the number of tests being performed. Note that quantiles
 270 are taken from different points as previously. If the correction is not applied, the
 271 first type error of the sequential test will grow uncontrolled. The step is repeated
 272 until there is no reasons to reject the null hypothesis and based on that stage pa-
 273 rameter L_k is selected.

274 In summary, the parameters estimation for the MAES algorithm is performed
 275 via the optimization of the following penalized likelihood

$$\log L_p(\theta) = \log L(\theta) - \gamma_1 p_1(\theta) - \gamma_2 p_2(\theta) \quad (8)$$

$$= \sum_{i=1}^n \log \left[\sum_{k=1}^K \pi_k \phi_k(\mathbf{x}_i | \boldsymbol{\mu}_k, \Sigma_k) \right] - \gamma_1 \sum_{p=1}^P \sqrt{\sum_{k=1}^K \pi_k \mu_{kp}^2} - \gamma_2 \sum_{k=1}^K \sum_{p=1}^P \max(\delta_{kp}, \epsilon_k) \quad (9)$$

276

277 3.3.2 Parameters estimation of the background

278 Estimation of the parameters involved in 8 is obtained via a suitable modification
 279 of the EM algorithm.

280 The component proportions of the Gaussian mixture components are expressed
 281 equally to the unpenalized case (equation 4).

282 Due to the shrinkage, the MPLE are shifted with respect to the MLE due to the
 283 shrinkage. The maximum penalized likelihood estimates are shifted with respect to
 284 the standard non-penalized estimates, and expressed as:

$$\hat{\mu}_{kp}^{(r+1)} = \begin{cases} 0 & \text{if } \left(\sum_{k=1}^K \left(\sum_{i=1}^n \tau_{ik}^{(r)} x_{ip} \right)^2 \right)^{\frac{1}{2}} \leq \gamma_1 M_p^{(r)} \\ \tilde{\mu}_{kp}^{(r+1)} - \gamma_1 \frac{\hat{\mu}_{kp}^{(r)} \Sigma_{k,pp}^{(r)}}{\|\hat{\mu}_p^{(r)}\| \sum_{i=1}^n \tau_{ik}^{(r)}} & \text{otherwise} \end{cases} \quad (10)$$

285 where $\tilde{\mu}_{kp}^{(r)}$ are the MLEs for the means given by equations 5 and $M_p^{(r)} = \max_{k=1,\dots,K} \hat{\Sigma}_{k,pp}^{(r)}$.
 286 Obviously, based on equation 10, for a sufficiently large γ_1 , all the mean components
 287 for the p^{th} variable are $\mathbf{0}$ when a given threshold is crossed.

288 Concerning the covariance matrices, denoted by $\tilde{\Sigma}_k^{(r)}$ the MLE estimates, eigen-
 289 value decomposition of $\tilde{\Sigma}_k^{(r)}$ is performed for each iteration r

$$\tilde{\Sigma}_k^{(r)} = \hat{Q}_k^{(r)} \tilde{D}_k^{(r)} \left(\hat{Q}_k^{(r)} \right)' \quad (11)$$

290 As no penalty is applied to component eigenvector matrix $\hat{Q}_k^{(r)}$, their penalized es-
 291 timates are the same as the MLEs. If the eigenvalues were shrunk to 0 then their
 292 MPLE of $\hat{D}_{k,pp}^{(r+1)}$ would be equal to $\tilde{D}_{k,pp}^{(r+1)}$ expressed as:

$$\tilde{D}_{k,pp}^{(r+1)} = \frac{-n\hat{\pi}_k^{(r+1)} + \sqrt{\left(n\hat{\pi}_k^{(r+1)}\right)^2 + 8\gamma_2 n\hat{\pi}_k^{(r+1)} \tilde{D}_{k,pp}^{(r)}}{4\gamma_2} \quad (12)$$

293 However, as the eigenvalues are shrunk to $\epsilon_k > 0$ then the sequential tests are per-
 294 formed based on which particular eigenvalue estimates $\hat{D}_{k,pp}^{(r+1)}$ are assigned either
 295 to be equal to ϵ_k or $\tilde{D}_{k,pp}^{(r+1)}$.

296 3.3.3 Variable selection for the background

297 Under assumption of component identity covariance matrices as considered by Pan
 298 and Shen [26], applied penalization leads to straightforward variable selection. If
 299 for all components the estimated mean value corresponding to the p -th variable is
 300 0 then the p -th variable is uninformative for cluster classification, hence should be
 301 removed from the considered data. This follows from equation 3 of the posterior
 302 probability of observation membership

$$\tau_{il} = \frac{\pi_l \phi(\mathbf{x}_i | \boldsymbol{\mu}_l, I_p)}{\sum_{k=1}^K \pi_k \phi(\mathbf{x}_i | \boldsymbol{\mu}_k, I_p)} = \frac{\pi_l \phi(x_{ip} | 0, 1) \phi(\mathbf{x}_{i,-p} | \boldsymbol{\mu}_{l,-p}, I_{p-1})}{\sum_{k=1}^K \pi_k \phi(x_{ip} | 0, 1) \phi(\mathbf{x}_{i,-p} | \boldsymbol{\mu}_{k,-p}, I_{p-1})} \quad (13)$$

303 where I_p is a diagonal matrix of dimension P and index $i, -p$ denotes the i^{th} vector
 304 with the removed p^{th} variable. After simplification of the equation it is clear that
 305 the observation for the p -th variable does not contribute to the classification based
 306 on the posterior probability.

307 For a more general case of the component-specific diagonal covariance matrix as
 308 in Xie [27], in order to remove the p -th variable the two conditions have to be met.
 309 The first one corresponds to mean estimates equal 0 as described above, while the
 310 second relies on the marginal component variances for a considered p -th variable

311 that should all be equal to 1 (due to data standardization). In that case, the posterior
 312 probability that an observation \mathbf{x}_i belongs to the l -th cluster is equal to

$$\tau_{il} = \frac{\pi_l \phi(\mathbf{x}_i | \boldsymbol{\mu}_l, \Sigma_l)}{\sum_{k=1}^K \pi_k \phi(\mathbf{x}_i | \boldsymbol{\mu}_k, \Sigma_k)} = \frac{\pi_l \phi(x_{ip} | 0, 1) \phi(\mathbf{x}_{i,-p} | \boldsymbol{\mu}_{l,-p}, \Sigma_{l,-p})}{\sum_{k=1}^K \pi_k \phi(x_{ip} | 0, 1) \phi(\mathbf{x}_{i,-p} | \boldsymbol{\mu}_{k,-p}, \Sigma_{k,-p})} \quad (14)$$

313 where notation $\boldsymbol{\mu}_{l,-p}$ denotes removal of p -th variable from the vector and $\Sigma_{l,-p}$ re-
 314 moval of p -th row and column from the matrix. In analogy to the previous case the
 315 p -th variable again does not contribute to the classification, hence it is uninforma-
 316 tive.

317 In the general case where the covariance matrix is not diagonal (hence also the
 318 correlations between variables are modeled) such a simple factorization cannot be
 319 performed. Without loss of the generality let us index all the features and take
 320 the two subsets $A = (1, \dots, L)$ and $B = (L + 1, \dots, P)$ for any $L \in [1, P - 1]$. The data
 321 and the respective parameters could now be partitioned into two sets as follows:
 322 $X = (X_A, X_B)$, component mean vectors $\boldsymbol{\mu}_k = (\boldsymbol{\mu}_{k,A}, \boldsymbol{\mu}_{k,B})$ and component covariance
 323 matrices are represented by the block matrices $\Sigma_k = \begin{pmatrix} \Sigma_{k,AA} & \Sigma_{k,AB} \\ \Sigma_{k,BA} & \Sigma_{k,BB} \end{pmatrix}$ where $\Sigma_{k,AB}$ is
 324 a block matrix constructed from Σ_k by taking rows from the set A and columns
 325 from the set B . The goal is to split the joint distribution of $f(X_A, X_B)$ into a marginal
 326 probability of X_B and a conditional probability for X_A . For equations 13 and 14 it
 327 was done almost in an automatic way because uncorrelated Gaussian distributions
 328 are conditionally independent.

329 From the factorization $f(X_A, X_B) = f(X_A | X_B) f(X_B)$ we could generalize equa-
 330 tion 14 and obtain the following formula:

$$\tau_{il} = \frac{\pi_l \phi(x_{iB} | \boldsymbol{\mu}_{l,B}, \Sigma_{l,BB}) \phi(x_{i,A} | \boldsymbol{\mu}_{l,A} + \Sigma_{l,AB} \Sigma_{l,BB}^{-1} (x_{i,B} - \boldsymbol{\mu}_{l,B}), \Sigma_{l,AA} - \Sigma_{l,AB} \Sigma_{l,BB}^{-1} \Sigma_{l,BA})}{\sum_{k=1}^K \pi_k \phi(x_{iB} | \boldsymbol{\mu}_{k,B}, \Sigma_{k,BB}) \phi(x_{i,A} | \boldsymbol{\mu}_{k,A} + \Sigma_{k,AB} \Sigma_{k,BB}^{-1} (x_{i,B} - \boldsymbol{\mu}_{k,B}), \Sigma_{k,AA} - \Sigma_{k,AB} \Sigma_{k,BB}^{-1} \Sigma_{k,BA})}. \quad (15)$$

331 The first necessary condition for removing set B of variables as uninformative
 332 for classification purpose is (as previously) to have 0 mean estimates for all the
 333 component means corresponding to the set B (for all $k = 1, \dots, K$ and $p \in B$ $\mu_{kp} = 0$).
 334 However, in contrast to the suggestion in Zhou et al. [28], the condition is not suf-
 335 ficient for considering the variables from the set B as uninformative. The posterior
 336 probability of observation membership if the first condition is met is

$$\tau_{il} = \frac{\pi_l \phi(x_{iB} | \mathbf{0}, \Sigma_{l,BB}) \phi(x_{i,A} | \boldsymbol{\mu}_{l,A} + \Sigma_{l,AB} \Sigma_{l,BB}^{-1} x_{i,B}, \Sigma_{l,AA} - \Sigma_{l,AB} \Sigma_{l,BB}^{-1} \Sigma_{l,BA})}{\sum_{k=1}^K \pi_k \phi(x_{iB} | \mathbf{0}, \Sigma_{k,BB}) \phi(x_{i,A} | \boldsymbol{\mu}_{k,A} + \Sigma_{k,AB} \Sigma_{k,BB}^{-1} x_{i,B}, \Sigma_{k,AA} - \Sigma_{k,AB} \Sigma_{k,BB}^{-1} \Sigma_{k,BA})}. \quad (16)$$

337 which implicitly is a function of the parameters modeling the distribution of the
 338 presumably uninformative variables, i.e. $\Sigma_{l,BB}$ and $\Sigma_{l,AB}$. Hence, in order to obtain
 339 a proper variable selection, the second condition relying on the covariance matrices
 340 has to be met (as shown later by the simulations).

341 The second necessary condition is to have component-wise equal correlations
 342 between variables from the set B , that is for all $k = 1, \dots, K$ $\Sigma_{k,BB} = \Sigma_{BB}$ and $\Sigma_{k,AB} =$
 343 Σ_{AB} . If both conditions are met for the set B then the posterior probability used for
 344 classification expressed formerly in 15 should be rewritten as

$$\begin{aligned}
 \tau_{il} &= \frac{\pi_l \phi(x_{iB}|0_B, \Sigma_{BB}) \phi(x_{iA}|\mu_{l,A} + \Sigma_{AB} \Sigma_{BB}^{-1} x_{iB}, \Sigma_{l,AA} - \Sigma_{AB} \Sigma_{BB}^{-1} \Sigma_{BA})}{\sum_{k=1}^K \pi_k \phi(x_{iB}|0_B, \Sigma_{BB}) \phi(x_{iA}|\mu_{k,A} + \Sigma_{AB} \Sigma_{BB}^{-1} x_{iB}, \Sigma_{k,AA} - \Sigma_{AB} \Sigma_{BB}^{-1} \Sigma_{BA})} \\
 &= \frac{\pi_l \phi(x_{iA}|\mu_{l,A} + \Sigma_{AB} \Sigma_{BB}^{-1} x_{iB}, \Sigma_{l,AA} - \Sigma_{AB} \Sigma_{BB}^{-1} \Sigma_{BA})}{\sum_{k=1}^K \pi_k \phi(x_{iA}|\mu_{k,A} + \Sigma_{AB} \Sigma_{BB}^{-1} x_{iB}, \Sigma_{k,AA} - \Sigma_{AB} \Sigma_{BB}^{-1} \Sigma_{BA})}. \tag{17}
 \end{aligned}$$

346 As a result the variables from set B influence the posterior distribution used for
 347 classification uniformly and independently on the true cluster membership. Hence
 348 if the two listed conditions are met, the variables from set B should be removed as
 349 uninformative for the dimensionality reduction purpose.

While the first condition is obtained automatically by shrinking the components mean vectors to 0, for the second condition a model selection has to be performed. Let the set A consist of all the features that do not meet the first condition and then the set B consists of the all potentially uninformative variables. Subsequently, let C be a set of all the possible subsets of set B ($C = C_1, \dots, C_{N_B}$ for an appropriate N_B index) and $D_i = C_i^C$ be the complements of sets C_i for $i = 1, \dots, N_B$. Iteratively, the N_B new models are created in a following way. For each i , the common blocks of component covariance matrices are computed as a weighted average of components blocks

$$\begin{aligned}
 \Sigma_{C_i C_i} &= \sum_{k=1}^K \pi_k \Sigma_{k, C_i C_i}, \\
 \Sigma_{D_i C_i} &= \sum_{k=1}^K \pi_k \Sigma_{k, D_i C_i}
 \end{aligned}$$

350 as it would be a sum of independent variables covariances. The idea is to substi-
 351 tute the component-specific blocks by the common one. The new model likelihood
 352 should be computed for each model. An information criterion is used to select the
 353 optimal model with features partitioned into sets of the uninformative variables C_i
 354 and the informative one D_i (i.e. the BIC criterion [35]).

355 The technique might seem computationally expensive, however, there is no need
 356 to fit $P!$ models. The first necessary criterion already filters out most of the true
 357 informative variables. There is also no need to check all the possible subsets of B
 358 as the minimal BIC values are likely obtained for models that are partitioned with
 359 subsets C_i with the highest cardinality.

360 3.3.4 Penalization of the background + signal model

361 The MAES algorithm and the associated data dimensionality reduction approach
 362 introduced above are the fundamental steps to obtain the background model and
 363 further to detect an unknown signal process. The developed anomaly detection
 364 algorithm (Penalized Anomaly Detection - PAD) integrates the penalized approach
 365 for the background density estimation and the fixed-background algorithm. The
 366 PAD algorithm introduces a penalty to the log-likelihood of the fixed-background
 367 model.

368 A form of the penalty should be chosen so that the proper variables are selected.
 369 A special care should be taken because the uninformative variables for the back-
 370 ground model could be possibly powerful for the signal/background discrimina-
 371 tion. Hence, the penalty should be a function of both the background and signal
 372 estimates. This in turn results in the dependence in estimation of the background
 373 and signal dependent parameters. The external loop iterates over the two-step pro-
 374 cedure of the fixed-background model to adopt the fixed background model idea to
 375 the penalized approach and the following variable selection.

376 The experimental data model is a mixture of $K + Q$ Gaussian components, from
 377 which the first K are estimated based on the background data X and the rest on
 378 the mixed data Y . The penalized log-likelihood to be maximized has the following
 379 form:

$$\begin{aligned}
 \log L_p(\theta|\theta(X)) = & \sum_{i=1}^m \log \left[(1 - \lambda) \sum_{k=1}^K \pi_k(X) \phi_k(\mathbf{y}_i | \boldsymbol{\mu}_k(X), \Sigma_k(X)) + \lambda \sum_{k=K+1}^{K+Q} \pi_k \phi_k(\mathbf{y}_i | \boldsymbol{\mu}_k, \Sigma_k) \right] \\
 & - \gamma_1(Y) \sum_{p=1}^P \sqrt{\sum_{k=1}^K \pi_k(X) \mu_{kp}(X)^2 + \sum_{k=K+1}^{K+Q} \pi_k \mu_{kp}^2} \\
 & - \gamma_2(Y) \sum_{p=1}^P \left(\sum_{k=1}^K \max(\delta_{kp}(X), \epsilon_k(X)) + \sum_{k=K+1}^{K+Q} \max(\delta_{kp}, \epsilon_k) \right),
 \end{aligned} \tag{18}$$

380 where $\theta(X)$ are the background model parameters, which are obtained by the max-
 381 imization of the penalized log-likelihood. When necessary in brackets it is denoted
 382 on which dataset (X or Y) the parameters depend. For the background estimation
 383 we consider slightly different penalized log-likelihood than in case of MAES algo-

384 rithm, i.e. the first penalty is also the function of the signal parameters:

$$\begin{aligned}
\log L_p(\theta|\theta(Y)) &= \sum_{i=1}^m \log \left[\sum_{k=1}^K \pi_k \phi_k(\mathbf{x}_i | \boldsymbol{\mu}_k, \Sigma_k) \right] \\
-\gamma_1(X) &\sum_{p=1}^P \sqrt{\sum_{k=1}^K \pi_k \mu_{kp}^2 + \sum_{k=K+1}^{K+Q} \pi_k(Y) \mu_{kp}(Y)^2} \\
-\gamma_2(X) &\sum_{p=1}^P \left(\sum_{k=1}^K \max(\delta_{kp}, \epsilon_k) \right),
\end{aligned} \tag{19}$$

385 where $\theta(Y)$ are the signal model parameters

386 Equation 18 differs from the penalized log-likelihood of the MAES algorithm
387 (equation 8) not only by the number of components that take part in the likelihood
388 formulation and penalty formulation. The optimization is based on the two separate
389 datasets and the penalty on the mean parameters is a joint function of all the back-
390 ground and signal components, hence it is not trivial to find the MPLE. Changes
391 in the estimates of the signal components influence the penalty value that in turn
392 impacts the estimates of the background density.

393 It is proposed to loop over the two-step procedure of the fixed background
394 model, i.e. optimize subsequently formulas 18 and 19 until the changes of param-
395 eters are negligible.

396 3.3.5 Parameters estimation of the background + signal model

397 The parameters estimation for the PAD algorithm is processed by a properly mod-
398 ified MAES algorithm. For simplicity let us first describe the two-step procedure
399 inside the outer loop. For the initialization, the simple background model should
400 be found and for this aim, the MAES algorithm described in the previous subsection
401 is applied. Subsequently, we need to find an estimate for the signal proportion λ
402 and the estimates for the component-specific parameters for the rest of the Q signal
403 components. In analogy to the MAES algorithm, the EM framework is employed.

404 First, the expectation step is computed for which posterior probabilities of clus-
405 ter membership is computed based on the already known and fixed background
406 components as:

$$\tau_{il}^{(r)} = \frac{\pi_l^{(r)} \phi(\mathbf{y}_i | \hat{\boldsymbol{\mu}}_l^{(r)}, \hat{\Sigma}_l^{(r)})}{\sum_{k=1}^{K+Q} \pi_k^{(r)} \phi(\mathbf{y}_i | \hat{\boldsymbol{\mu}}_k^{(r)}, \hat{\Sigma}_k^{(r)})}. \tag{20}$$

for l in $K+1, \dots, K+Q$ (the signal components). The formulas for signal parameters 4, 5, 6, 11 and 12 remain unchanged but the iterations of the estimates are computed based on the Y dataset. The proportion of signal events λ is equal to $\sum_{k=K+1}^{K+Q} \pi_k$.

Given the proportion estimate $\hat{\lambda}$ the known background components proportions should be rescaled so that $\sum_{k=1}^{K+Q} \pi_k = 1$, that is to apply a transformation:

$$\pi_k^{(r+1)} = \frac{\pi_k^{(r+1)}}{\sum_{k=1}^K \pi_k^{(r)}} * (1 - \hat{\lambda})$$

407 for $k = 1, \dots, K$.

408 The MPLE for the signal means are expressed as

$$\hat{\mu}_{kp}^{(r+1)} = \begin{cases} 0 & \text{if } \left(\sum_{k=1}^K \left(\sum_{i=1}^n \tau_{ik}^{(r)} y_{ip} \right)^2 \right)^{\frac{1}{2}} \leq \gamma_1 M_p^{(r)} \\ \tilde{\mu}_{kp}^{(r+1)} - \gamma_1 \frac{\hat{\mu}_{kp}^{(r)} \Sigma_{k,pp}^{(r)}}{\|\hat{\mu}_{\cdot p}^{(r)}\| \sum_{i=1}^n \tau_{ik}^{(r)}} & \text{otherwise} \end{cases} \quad (21)$$

409 for $k = K + 1, \dots, K + Q$ where $M_p^{(r)} = \max_{k=1, \dots, K+Q} \hat{\Sigma}_{k,pp}^{(r)}$. Note that the norm $\|\hat{\mu}_{\cdot p}^{(r)}\|$
 410 should be computed based on all the $K + Q$ components.

411 Finally, the outer loop should iterate over the explained above fixed-background
 412 estimation procedure. During the subsequent iteration, the MAES model is fitted
 413 to the background data with the slight change. Instead of equation 10 the formula
 414 21 for components $k = 1, \dots, K$ should be used in order to borrow the knowledge of
 415 the already found signal components. After the background is refitted the second
 416 step of the anomaly detection should be performed. As a result, the background
 417 mean estimates from the initial step (even the one that had been shrunk to 0) could
 418 change if a significant signal is present in the mixed data.

419 4 Experimental analysis on toy simulated data

420 4.1 Goals of the analysis

421 Collections of artificial data were generated in order to understand the performance
 422 of the proposed methodology in terms of classification in an unsupervised setting
 423 (i.e. to estimate the background distribution) and in a semi-supervised setting (to
 424 find a signal process). The simulations touch different aspects of the algorithm per-
 425 formance with respect to:

- 426 • Different implementations of the proposed approach to handle variable se-
 427 lection. Within the penalized model-based clustering approach we consider
 428 and test two different scenarios to perform variable selection. The first (M1)
 429 is a natural result for the MAES algorithm described above and the model is
 430 obtained by a model fit to the data of the full dimension P . The used penal-
 431 ties serve as regularization and variable selection. The second implementation

432 (M2) also relies on the MAES algorithm but is constructed in two passes. First
 433 the regular MAES is fitted to data of the full dimension P as the mean for
 434 variable selection. In the second pass the model is fitted again but based only
 435 on informative variables that had been selected in the former pass. The M2
 436 model is expected to have better prediction performance because in the re-
 437 duced space of informative variables smaller penalty (or even none at all)
 438 should be applied to the data. This results in smaller bias of the parameter
 439 estimates and as well the estimates are more stable. On the other hand, this
 440 approach might suffer from a possible error propagation and a decrease of
 441 classification performance if some of the informative variables are incorrectly
 442 removed. For the simulation setting, when MAES is mentioned it is assumed
 443 that the M1 method is used because it is a natural consequence of the penal-
 444 ized approach. The M2 method has less theoretical bases, could suffer from er-
 445 ror propagation and is against the paradigm of joint parameter estimation and
 446 variable selection, however it is worth to test and compare its performance.

- 447 • Comparison with the competing models, i.e. the parsimonious family of mod-
 448 els introduced in Fraley and Raftery [17] and also Bouveyron et al. [22], ap-
 449 plication of the PCA prior to the parameter estimation according to Kuusela
 450 et al. [16] and the penalized log-likelihood approach of Pan and Shen [26].
- 451 • Varying configurations of the background and possible signal. For this reason,
 452 evaluation has considered different degrees of separation between the mixture
 453 components and different mixing proportions of the components.

454 4.2 Simulation settings

455 The simulated data are generated from mixtures of a few Gaussian distributions as
 456 a proof of concept to enable easier analysis for simple examples. Additionally, the
 457 true parameters of the generating model are chosen so that the particular features
 458 of the algorithm performance could be explored.

For the background data the following model has been considered:

$$f_B(\mathbf{x}) = \sum_{k=1}^K \pi_k \phi(\mathbf{x} | \boldsymbol{\mu}_k, \Sigma_k),$$

459 where

- 460 • K is chosen in $\{2, 3\}$.
- Mean vectors are set as $\boldsymbol{\mu}_k = (1, \dots, 1, 0, \dots, 0)'$ * *mult* with

$$mult = \begin{cases} (m, -m) & \text{for the } K = 2 \text{ setting} \\ (m, 0, -m) & \text{for the } K = 3 \text{ setting} \end{cases}$$

461 for m in $\{0.1, \dots, 0.8\}$ and $\sum_{p=1}^P \boldsymbol{\mu}_{kp} = \frac{P}{2} \text{mult}$.

- Covariance matrices are set as

$$\Sigma_k = \begin{pmatrix} \Sigma_{k1} & 0 & 0 \\ 0 & \Sigma_{k1} & 0 \\ 0 & 0 & I_8 \end{pmatrix}$$

where $\Sigma_{k1} = P_k D_k P_k'$ with

$$P_1 = \begin{pmatrix} 1 & 0 & -1 & 1 \\ 1 & \sqrt{2} & 1 & 0 \\ 1 & -\sqrt{2} & 1 & 0 \\ -1 & 0 & 1 & 2 \end{pmatrix}, \quad P_2 = \begin{pmatrix} -1 & 0 & 1 & 1 \\ 1 & -\sqrt{2} & 1 & 0 \\ 1 & \sqrt{2} & 1 & 0 \\ 1 & 0 & -1 & 2 \end{pmatrix}, \quad P_3 = I_{\frac{P}{4}}$$

$$D_1 = \begin{pmatrix} 1 & 0 & 0 & 0 \\ 0 & 0.5 & 0 & 0 \\ 0 & 0 & 0.15 & 0 \\ 0 & 0 & 0 & 0.12 \end{pmatrix}, \quad D_2 = \begin{pmatrix} 1 & 0 & 0 & 0 \\ 0 & 0.1 & 0 & 0 \\ 0 & 0 & 0.4 & 0 \\ 0 & 0 & 0 & 0.1 \end{pmatrix}, \quad D_3 = I_P$$

- Component proportion are set to

$$\pi = \begin{cases} (0.5, 0.5) & \text{for the } K = 2 \text{ setting} \\ (0.5, 0.3, 0.2) & \text{for the } K = 3 \text{ setting} \end{cases}$$

- 462 • Data sizes n in $\{250, 500\}$ and dimension $P = 16$.

463 Given this set of the parameters the variables 9 – 16 are truly uninformative.

464 For anomaly detection simulations, the background data are generated using
 465 $K = 2$ Gaussian components with parameters specified as above. The signal process
 466 is simulated by a single Gaussian component with parameters specified as for the
 467 third background component described above. The experimental data is generated
 468 for different proportions of signal events λ in $\{0.2, 0.1, 0.05\}$. The generated back-
 469 ground and experimental data sizes are $n = m = 500$. As the signal component is
 470 placed between the background components, for testing purpose (when it is speci-
 471 fied), the signal mean for the 14th variable (which is uninformative in respect to the
 472 background set) is specified to be non-zero.

473 4.3 Details

- 474 1. The simulations were performed in R environment for statistical computing
 475 [36] version 3.4.2.
- 476 2. Competing approaches for the model-based clustering of the background data

- 477 • Model-based clustering without any restriction on constraint on the co-
478 variance parametrization based on the Fraley and Raftery [17] with the
479 associated implementation [37].
- 480 • Model-based clustering approach using the unrestricted component co-
481 variance matrices with prior reduction of the data dimension to the first
482 two principal components as proposed in [15, 16]
- 483 • A family of parsimonious mixture models as proposed in Bouveyron et al.
484 [22] and implemented in the HDclassif R package [38].
- 485 • A penalized approach of Pan and Shen [26] with component covariances
486 restricted to identity matrices.

3. Model selection - an important aspect of a model-based clustering and the penalized approach is proper determination of the number of Gaussian components K that should be used for modeling and as well the values for the regularization parameters γ_1 and γ_2 . The commonly used approach for the unpenalized mixtures model is to use the Bayesian Information Criteria (BIC) which was defined by Schwarz [35] as

$$BIC_1 = -2\log L(\hat{\theta}) + \log(n) * d,$$

where d is the number of free parameters in the model, L is the model likelihood and $\hat{\theta}$ are the MLE. According to the criterion a model that minimizes the BIC should be selected as an optimal trade off between the goodness of fit and the model complexity. However for the penalized model some parameters are shrunk and should not be considered any longer as free. Following Pan and Shen [26] and Bühlmann and Van De Geer [32] motivated by a study in context of the penalized regression of Efron et al. [24] a modified BIC criterion could be used. It is formulated as

$$BIC_2 = -2\log L(\hat{\theta}) + \log(n) * d_{eff},$$

487 where d_{eff} is the effective number of parameters (parameters not shrunk
488 to the fixed value) and $\hat{\theta}$ are MPLE. Despite the lack of rigorous theoretical
489 arguments justifying the use of the modified BIC criterion, practically in sim-
490 ulations and application the criterion serves very well.

491 In practice, the minimum value for the BIC is found based on an extensive
492 grid search over the parameters space. In a first phase the grid is coarse and
493 later the search is performed on a more compacted grid trimmed appropri-
494 ately based on the previous pass. With special care the grid boundaries are
495 chosen in order to select the global minimum for BIC function not only the
496 local one. BIC values are discontinuous with respect to regularization param-
497 eters, however as they increase sufficiently the associated BIC values are so

498 large, that it is clear that the global minimum should be found for lower regu-
499 larization parameters. Based on this observation the grid points are set.

500 For the considered simulation for all the models, we consider that the number
501 of Gaussian components is known a priori, so that the results are not influ-
502 enced by incorrect specification of K .

503 4. Performance evaluation of the model-based clustering methods are based on
504 the Adjusted Rand Index [39]. In general the Rand Index is a measure of ac-
505 curacy of correctly classified observations [40]. The adjusted version corrects
506 value of the former Rand Index so that for a random classification the expected
507 index value is equal to 0.

508 5. It should be noted that the EM algorithm does not guarantee to find the cor-
509 rect maximum of the objective function (penalized log-likelihood) as it could
510 find one of local maxima. It strongly depends on the starting values and for
511 this reason the algorithm should be run a few times from the different initial-
512 ization points $\pi_k^{(0)}$, $\mu_k^{(0)}$ and $\Sigma_k^{(0)}$ for $k = 1, \dots, K$. Additionally, maximization of
513 the log-likelihood function of the Gaussian mixture model is not a well-posed
514 problem, i.e. the likelihood tends to the infinity if one of the components be-
515 comes a singularity that models a single observation. These issues become
516 more apparent especially for the datasets with a higher number of dimen-
517 sions. For these reasons, the algorithm is run from many starting points and a
518 stopping rule is implemented if the algorithm does not converge.

519 For the grid search it is clever to use the so-called warm-starts as initialization
520 values, i.e. the estimates of the model with smaller regularization parameters.
521 For new regularization parameters the MPLE are not far from the previous
522 run, hence it is often sufficient to run the algorithm from a single starting
523 point. Given the warm-start the algorithm converges much faster (in about 10
524 iterations versus about 50 needed for arbitrary starting points) and does not
525 need to be run multiply times.

526 6. Note that the datasets X and Y could differ in size and prior distribution they
527 have been produced. For this reason, regularization parameters γ_1 and γ_2
528 should be selected separately for each of them. We propose to select the regu-
529 larization parameters for the background once (despite the further loop itera-
530 tions) when the initializing background model is obtained. The regularization
531 parameters for the second stage of the PAD algorithm and the number of sig-
532 nal components Q should be found using a grid search and an optimization
533 criterion.

534 **4.4 Results and comments**

535 **4.4.1 Model-based clustering**

536 Let us consider a scenario where the data are generated from the Gaussian mix-
537 ture with two equally weighted components and parameters specified as described
538 above.

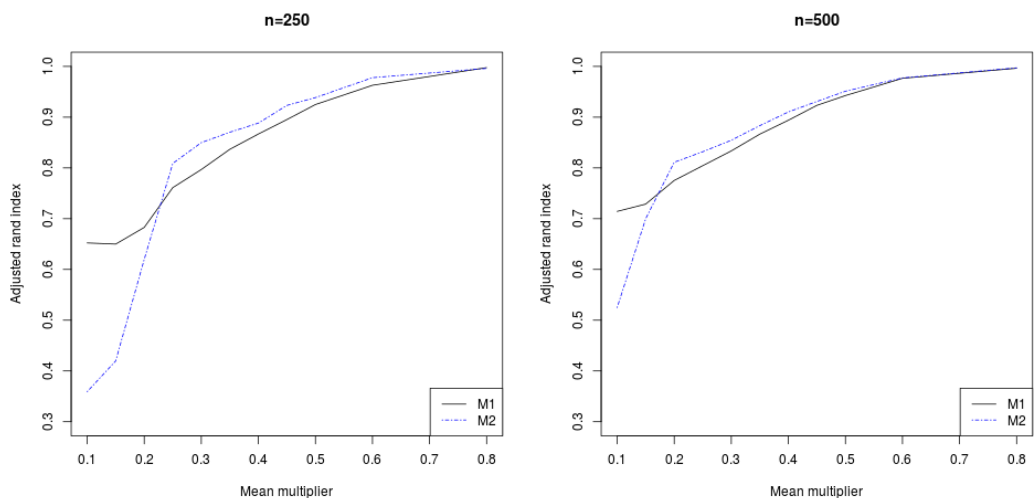


Figure 1: Performance comparison for the two types (M1 and M2) of variable selection methods for the proposed model-based clustering algorithm for the data of size $n = 250$ and $n = 500$ with different values of the mean multiplier. The results are based on the average performance on 30 simulated datasets.

539 Comparison of variable selection methods (figure 1) for MAES suggests that the
540 M2 model performs best in terms of the adjusted Rand index. However, for the
541 small components separation and $n = 250$, the variable selection methodology in-
542 correctly removes the informative variables. This decreases the performance of the
543 M2.

544 For the simple scenario of the balanced data the introduced MAES algorithm has
545 as superior performance in comparison to the other methods (figure 2), especially
546 for the data with the lowest size $n = 250$ and small true components separation (the
547 most difficult cases). As the separation increases and classification becomes easier,
548 all but the method of Vatanen et al. [15] have comparable performance. Inferior
549 performance of Vatanen et al. [15] method is presumably due to improper variable
550 selection as for this case the first two principal components explain only a small
551 fraction of the total variability.

552 Subsequently, let us consider scenario when the data are generated from the
553 Gaussian mixture with 3 components and parameters as specified at the beginning
554 of the section. In this case mixture components are of different proportions and this
555 is an additional difficulty affecting the performance of clustering algorithms.

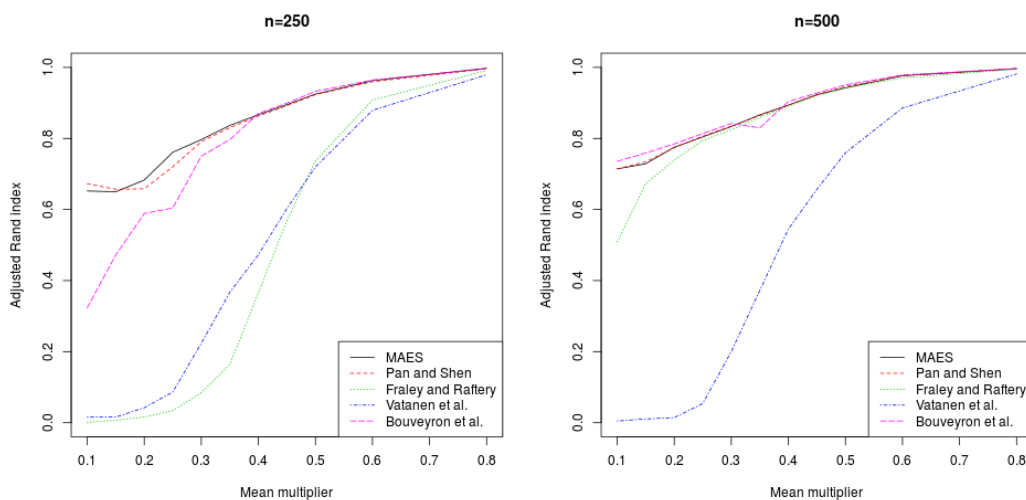


Figure 2: Performance comparison for the 5 model-based clustering methods for the data of size $n = 250$ and $n = 500$ for different values of mean multiplier $mult$ (true separation of classes).

556 In comparison to the previous simulations where the components had equal pro-
 557 portions, for 3 unbalanced components we naturally observe much lower scores of
 558 the adjusted Rand index. Performance for variable selection approaches (models
 559 M1 and M2) presented above supports the M2 approach (figure 3). The hierarchy of
 560 model performances changes slightly between the balanced and unbalanced scenar-
 561 ios, but MAES, Pan and Shen and Bouveyron et al. are still leading, especially for
 562 the larger data size (figure 4). For the smaller data size and small separation MEAS
 563 algorithm has far better performance than the competing models.

564 4.4.2 Anomaly detection

565 For anomaly detection simulations the respective background and experimental
 566 (background + signal) datasets are respectively with distributions specified in sub-
 567 section 4.2. Each pair of datasets is properly transformed. The background data
 568 are standardized according to their sample mean and variance. The experimental
 569 data are standardized as well but according to the background sample mean and
 570 variance, hence in general mixed data mean is different from 0 especially if a strong
 571 signal is present.

572 The simulations are performed as follow. First, for signal fraction $\lambda = 5\%$ the
 573 anomaly detection algorithm is run for varying $mult$ parameter (separation of the
 574 background components). The results are presented in the first three rows of table
 575 1. For the high components separation, there is no problem in signal/background
 576 classification however for $mult = 1$ the signal misclassification error raises to 76%.
 577 In row 4 and 5 is presented the performance for higher signal proportion in the ex-

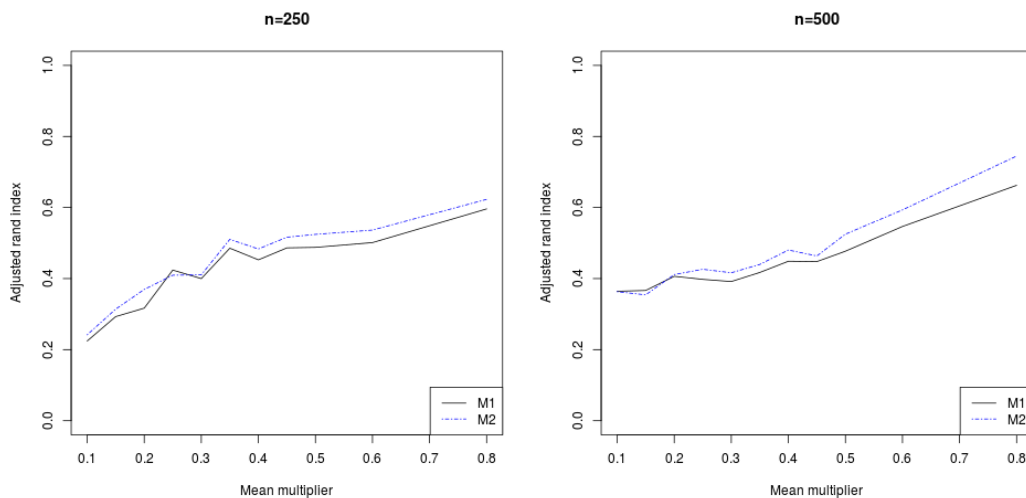


Figure 3: Performance comparison for the two types (M1 and M2) of variable selection methods for the proposed model-based clustering algorithm for the data of size $n = 250$ and $n = 500$ with different values of the mean multiplier. The results are based on the average performance on 30 simulated datasets.

578 perimental data by having fixed separation. Only the high signal proportion allows
 579 for a decrease of the misclassification error. For the next three following simula-
 580 tions, the true signal means for the 14th variable (which is uninformative according
 581 to background data) is changed from 0 to 3, so that the signal strongly exhibits as
 582 a deviation from the background distribution. This results in much better signal
 583 classification. It is due to the fact that true signal observations lie between the high
 584 background distribution probability domain. Figure 5 presents the fitted density to
 585 the mixed data. Hence the signal classification error is not as low as one could wish,
 586 but the signal component is estimated close to the true one.

587 Finally, the feature space was reduced according to both criteria described above
 588 and a new model was refitted in the reduced space (M2 model approach). The re-
 589 sults are presented in the last 6 rows of table 1. In each case, the Adjusted Rand In-
 590 dex for classification is increased with respect to the approach without dimensional
 591 reduction. The improvement is a result of smaller bias caused by penalty function
 592 applied to all the informative and uninformative variables. After dimensionality
 593 reduction the penalty is much softer (or even not present) as the uninformative
 594 variables could not be present in the data any more.

595 4.5 Simulation conclusions

596 In unsupervised setting, the MAES algorithm was tested against the competitors to
 597 access classification performance. Half of the variables of the simulated data were
 598 taken as uninformative, which favors the proposed algorithm which employs vari-

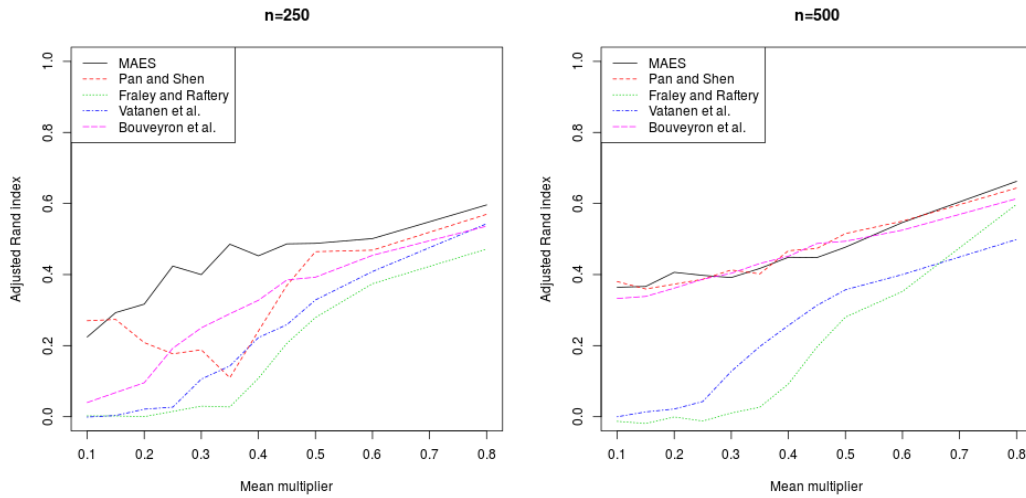


Figure 4: Performance comparison for the 5 model-based clustering methods for the data of size $n = 250$ and $n = 500$ for different values of mean multiplier $mult$ (true separation of classes). By MAES is always understood the M1 variable selection model for clarity (despite superior performance of M2 for the given simulation schema).

599 able selection jointly with parameter estimation. For this reason Fraley and Raftery
 600 [17] and Vatanen et al. [15] approach turns out to perform worst. Difference be-
 601 tween algorithm performance is most visible for the most difficult cases that sup-
 602 port the MAES. For easier cases or for bigger data the algorithms tend to perform
 603 similarly.

604 We considered two methods for variable selection (M1 and M2). The simulations
 605 favour M2 model, it has superior performance versus M1, unless the background
 606 components are hardly separated from each other, which results in the removal of
 607 informative variables and a consequent worsening of the performance.

608 For semi-supervised anomaly detection, the PAD algorithm is robust against the
 609 separation of the background and signal components. It was presented that if for
 610 some uninformative variable according to the background data a strong signal is
 611 exhibited ($\mu_{s,14} = 3$), then the variable is not removed and classification is improved.
 612 Finally, the M2 method was shown to perform better than the M1 for all the tested
 613 cases. We presume that the high penalty used for removing many of uninformative
 614 variables causes bias on other parameters leading to poorer classification.

615 The PAD algorithm was compared with the Kuusela et al. [16] approach for
 616 which the simulated data is reduced to the first two principal components. For
 617 the given case, the first two components represent only 21% of total data variabil-
 618 ity. In order to be able to explain at least 80% of the total variability 11 principal
 619 components (out of 16) should be selected. Hence, taking only the first two compo-
 620 nents puts under the risk that any possible signal deviation is omitted by the PCA

Table 1: Anomaly detection results compared for varying background distribution, signal fraction λ and signal true mean μ_s . Also the dimension reduction technique (model M2) is applied and its results are shown in the last 6 rows. There are 8 uninformative variables, but true signal mean vector is equal to $\mathbf{0}$ (unless the signal mean for the 14th variable ($\mu_{s,14}$) is increased to 3).

| $\mu_{s,14}$ | <i>mult</i> | λ | model | misclassified events | misclassified signal events | Rand Index | misclass. error |
|--------------|-------------|-----------|-------|----------------------|-----------------------------|------------|-----------------|
| 0 | 2 | 0.05 | M1 | 0 | 0 | 1.000 | 0.000 |
| 0 | 1.5 | 0.05 | M1 | 15 | 0 | 0.937 | 0.030 |
| 0 | 1 | 0.05 | M1 | 19 | 19 | 0.926 | 0.038 |
| 0 | 1 | 0.10 | M1 | 42 | 42 | 0.839 | 0.084 |
| 0 | 1 | 0.20 | M1 | 37 | 20 | 0.825 | 0.074 |
| 3 | 1 | 0.05 | M1 | 18 | 18 | 0.929 | 0.036 |
| 3 | 1 | 0.10 | M1 | 22 | 21 | 0.908 | 0.044 |
| 3 | 1 | 0.20 | M1 | 14 | 8 | 0.928 | 0.028 |
| 0 | 1 | 0.05 | M2 | 13 | 13 | 0.948 | 0.026 |
| 0 | 1 | 0.10 | M2 | 15 | 14 | 0.936 | 0.030 |
| 0 | 1 | 0.20 | M2 | 17 | 15 | 0.897 | 0.034 |
| 3 | 1 | 0.05 | M2 | 8 | 7 | 0.967 | 0.016 |
| 3 | 1 | 0.10 | M2 | 8 | 7 | 0.964 | 0.016 |
| 3 | 1 | 0.20 | M2 | 11 | 9 | 0.945 | 0.022 |

621 procedure. Indeed, in table 2 we see that the algorithm proposed by Kuusela et al.
622 has better performance in terms of Rand index for $\mu_{s,14} = 0$ than for $\mu_{s,14} = 3$ - that
623 is the case when signal distribution diverge more from the background (rather the
624 opposite behavior one would expect). The PAD algorithm of M1 type has slightly
625 worse performance for $\mu_{s,14} = 0$ than Kuusela’s but better for $\mu_{s,14} = 3$. However,
626 the PAD algorithm of M2 type is superior to others for all the tested cases.

627 **5 Application to a model-independent search for new** 628 **physics**

629 For a proof of concept of the method in the context of a physics analysis, we have
630 produced simulated datasets. Specifically, we are interested in the signature con-
631 taining two jets in the final state (known also as “dijet” final states), denoted as “jj”
632 coming from proton-proton collisions at the LHC; for such signatures, background
633 and hypothetical signal collision events have been generated as described below. A
634 simple analysis selection is then performed on the samples and finally the anomaly
635 detection method is tested.

Table 2: Anomaly detection results based on the algorithm introduced by Kuusela et al. [16] for the data reduced to the first two principal components. The simulation is performed against varying signal fraction λ and signal true mean μ_s . For comparison reasons, adjusted Rand indexes for PAD algorithm for both M1 and M2 models are also included.

| $\mu_{s,14}$ | <i>mult</i> | λ | misclass. events | misclass. sig. events | Rand Index | PAD M1 Rand Index | PAD M2 Rand Index | classif. error |
|--------------|-------------|-----------|------------------|-----------------------|------------|-------------------|-------------------|----------------|
| 0 | 2 | 0.05 | 3 | 3 | 0.987 | 1.000 | - | 0.006 |
| 0 | 1.5 | 0.05 | 8 | 8 | 0.967 | 0.937 | - | 0.016 |
| 0 | 1 | 0.05 | 17 | 17 | 0.932 | 0.926 | 0.948 | 0.034 |
| 0 | 1 | 0.10 | 24 | 22 | 0.899 | 0.839 | 0.936 | 0.048 |
| 0 | 1 | 0.20 | 34 | 22 | 0.838 | 0.825 | 0.897 | 0.068 |
| 3 | 1 | 0.05 | 25 | 25 | 0.902 | 0.929 | 0.967 | 0.050 |
| 3 | 1 | 0.10 | 30 | 28 | 0.877 | 0.908 | 0.964 | 0.060 |
| 3 | 1 | 0.20 | 41 | 33 | 0.811 | 0.928 | 0.945 | 0.082 |

636 5.1 MC samples

637 We generated a set of MC samples using standard simulation software for high-
638 energy collisions. The simulated phenomena correspond to proton-proton colli-
639 sions at a center-of-mass energy $\sqrt{s} = 13$ TeV and measured by a simplified AT-
640 LAS detector simulation implemented in the DELPHES package. The main source of
641 Standard Model (SM) background in our signature is the production of two jets via
642 QCD processes, namely from the production of a pair of gluons, a pair of quarks,
643 or a gluon and a quark. The simulated signal corresponds to the production of
644 a stop quark decaying into two jets, in the R-parity violating Minimal Supersym-
645 metric Model (RPV-MSSM) [41, 42], using the package in [43]. A more in-depth
646 description of the simulations performed for signal and background follows.

647 5.1.1 Signal

648 As a benchmark for testing the anomaly detection algorithm, we produced a sample
649 of $5 * 10^5$ stop quark signal events. The hard process was simulated using MAD-
650 GRAPH 5, where we used the four-flavor scheme and nn231o1 [44] to model the
651 proton PDFs. The resulting events were then ported to PYTHIA 8.230 for shower-
652 ing, decay and hadronization. All default parameters from MADGRAPH 5.2.6.0 were
653 used except the value of the pseudorapidity, restricted to $|\eta| < 2.5$.

654 Within the RPV-MSSM model used, the production and decay (to two jets) of
655 a resonant stop happens via a single Feynman diagram in a four-flavor scheme, as
656 depicted in figure 6.

657 The production cross section reported by MADGRAPH 5 is 18.011 ± 0.003 pb.

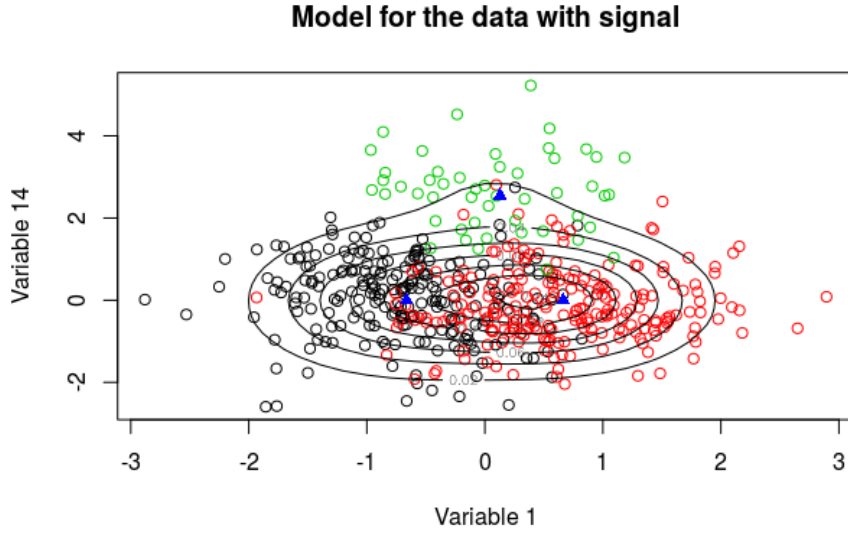


Figure 5: Estimated distribution for the the mixed data with signal fraction $\lambda = 5\%$ and the true signal mean for the 14^{th} variable increased to 3. The blue triangles are estimated Gaussian mean components. The plot shows the mixed data in space spanned by the 1^{st} and 14^{th} transformed variable. Green point correspond to signal, while black and red to the background components.

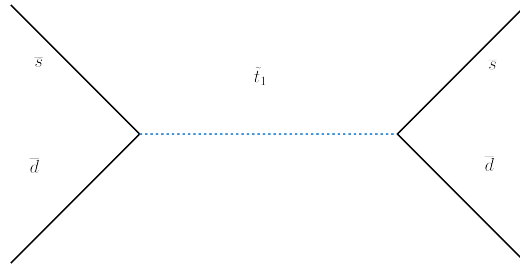


Figure 6: Feynman diagram for the production of a stop quark decaying into two light quarks, in the RPV-MSSM [41, 42].

658 5.1.2 Background

659 The production of $5 * 10^5$ dijet events from QCD processes was performed using the
 660 same MADGRAPH 5 and PYTHIA 8 versions as the ones for the signal. There are many
 661 ways in which QCD interactions can lead to a pair of jets in the hard process, namely
 662 all possible diagrams that contain two gluons, a quark and a gluon or two quarks
 663 in the final state. In a four-flavor scheme at tree level, there are 65 such processes.
 664 The production cross section corresponding to the QCD background reported by
 665 MADGRAPH 5 is: 3.382 ± 0.001 mb.

666 5.1.3 Detector simulation

667 Both signal and background event samples have been passed through a fast detector
668 simulation using the DELPHES 3.4.1 software. We have kept all default parameters
669 except the jet cone parameter $\Delta R = 0.4$, and used the ATLAS detector card that
670 comes with the software distribution.

671 5.2 Event selection

672 The signal and background simulated samples are then analyzed and an event se-
673 lection is applied. A set of requirements are imposed on the object properties and
674 event variables, inspired by realistic experimental analyses, in order to e.g. mitigate
675 detector effects, simulate trigger selection. Furthermore, several features (variables)
676 are extracted and calculated. The features of the events that pass the selection com-
677 prise the input of the anomaly detection algorithm. Typical values of object selec-
678 tion are already included in the DELPHES ATLAS detector card; at this level, the only
679 additional requirement we impose is that the event contains only two jets and each
680 of them has a transverse momentum of 20 GeV or more.

681 Given that we are performing a model-independent search, the selection re-
682 quirements are not optimized for any particular signal, even if we could, in princi-
683 ple, devise such a procedure for the stop production described above.

684 The variables extracted and calculated for each event are the following:

- 685 • Transverse momentum for each of the jets: $p_T(j_1), p_T(j_2)$.
- 686 • Reconstructed invariant mass of the dijet system: $M_{\text{inv}}(j_1, j_2)$.
- 687 • Missing transverse energy: E_T^{miss} .
- 688 • Angular distance of the two jets in the $\eta - \phi$ plane: $\Delta R(j_1, j_2)$.
- 689 • Sphericity and centrality, as defined in [45].

690 Normalized distributions for the background and signal described above can be
691 found in figure 7.

692 5.3 Method performance

Marginal distributions for the produced background and signal samples are uni-
modal and most of them stand out to be heavily skewed. Certainly, skewed distri-
butions could be approximated by the Gaussian mixtures but this requires to use
many components that could lead to over-parametrization. Hence to obtain a more
accurate model, there is a need for proper data transformation, so that the marginal
variables distributions are as close to the normal distribution as possible. For this
reason, Tukey's Ladder of Powers transformation is applied for each variable of the

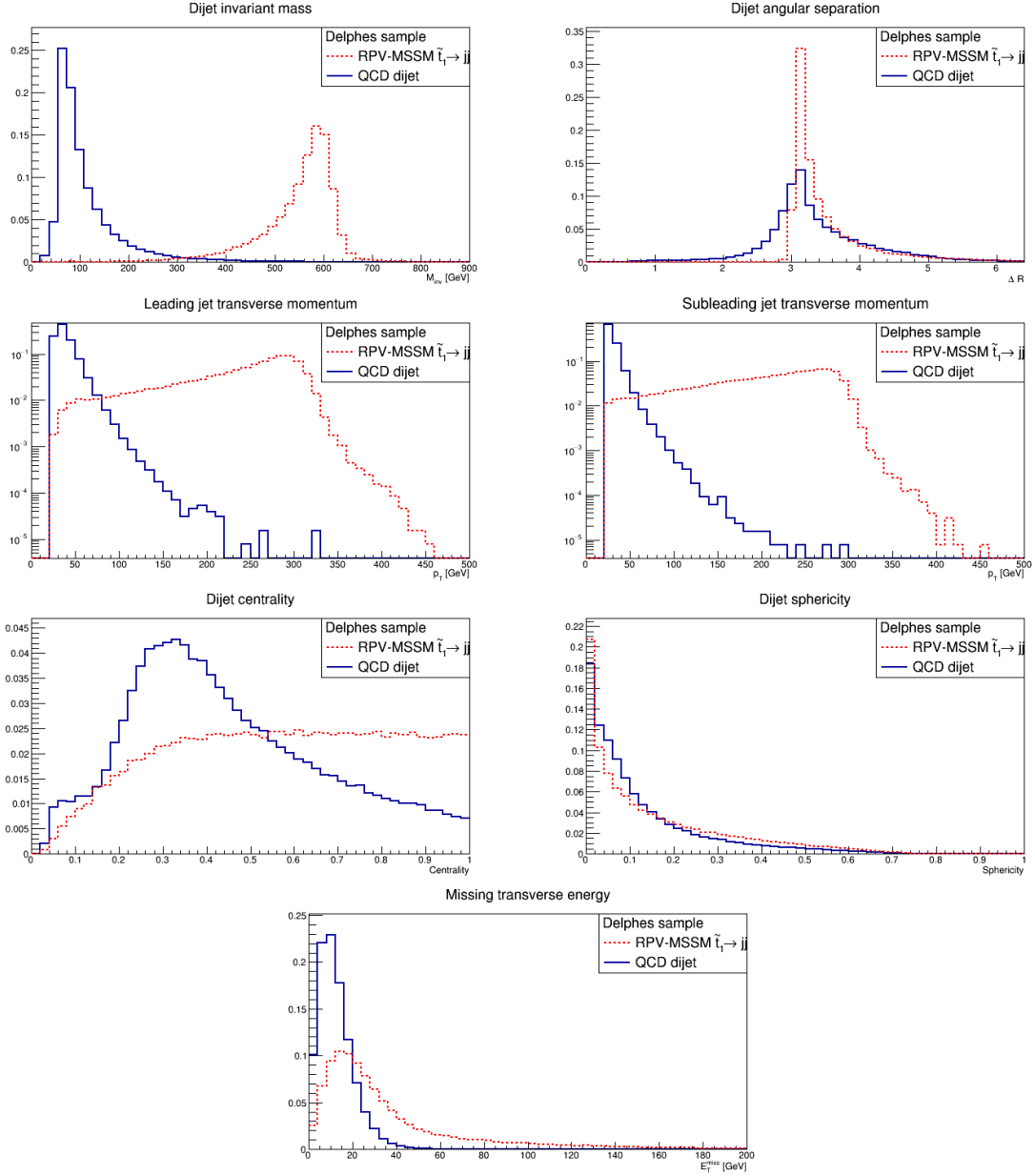


Figure 7: Normalized distributions of signal and dijet background for seven kinematic and angular variables.

background data subsequently [46, 47]. Formally, separate transformations are applied to each variable based on a properly chosen parameter ρ_k , that is:

$$x_{ik}^* = \begin{cases} x_{ik}^{\rho_k} & \text{if } \rho_k > 0 \\ \log(x_{ik}) & \text{if } \rho_k = 0 \\ -x_{ik}^{\rho_k} & \text{if } \rho_k < 0 \end{cases}$$

693 for $i = 1, \dots, n$ and ρ_k selected separately for each k in $1, \dots, K$. Parameter ρ_k is se-
694 lected based on the background and the same transformation is applied to simu-
695 lated experimental data which are a mixture of the background and signal events.
696 Afterwards, the background data are scaled according to their sample mean and
697 variance. Scaling is also applied to the experimental sample but according to the
698 sample mean and variance of the background.

699 Although the univariate background data distributions after the transformations
700 are unimodal and resemble Gaussian, it would be an oversimplified model if the
701 background density would be estimated by a single multivariate Gaussian com-
702 ponent. If the 2-dimensional data distributions are analyzed, they do not exhibit
703 elliptical Gaussian shape. One reason for this is preprocessing of the produced col-
704 lision events from which only a group of potentially interesting are selected. Also
705 ordering of event variables (i.e. $p_T(j_1) \geq p_T(j_2)$) introduces strict limits onto fea-
706 ture space. Finally the background is produced by many underlying processes that
707 results in complex distribution. For this reasons the background distribution needs
708 to be modelled by a mixture of many components.

709 The data subset of size $n = 4000$ was taken from the background sample. The
710 optimal number of Gaussian components to model the background was selected to
711 be equal to 10 based on the described modified BIC criteria. In total there are 359
712 parameters to be estimated. Due to the background complexity, the regularization
713 parameter γ_1 was chosen to be 0, hence all the variables play an important role in
714 the model-based clustering. The second regularization parameter γ_2 is positive and
715 plays an important role for component covariance matrices regularization. As the
716 first necessary condition for variable selection cannot be met, the approaches for
717 variable selection (M1 and M2) are equivalent.

718 The background model serves as an initialization point for the PAD algorithm.
719 However for $\gamma_1 = 0$, subsequently found signal components do not influence the
720 background estimation through the penalty, hence the PAD algorithm is reduced
721 to the fixed-background model with regularization on the component covariance
722 matrices.

723 For the varying proportion of signal observations λ in the experimental data, the
724 PAD algorithm is tested. For each λ , 50 datasets of size $n = 4000$ are sampled from
725 the respective background and signal datasets so that the simulated experimental
726 data are constructed. In following, we search only for a single signal component.
727 This is an already challenging task, and its results are sufficient to provide insight
728 in the possible presence of an anomalous process in the data.

729 The algorithm is able to find and estimate a signal component corresponding to
730 an unknown process not present in the background data for the signal proportion
731 $\lambda = 0.05$ without any problem. However, for smaller signal proportion λ problems
732 start to arise. For many algorithm runs estimates for the signal proportion $\hat{\lambda}$ is
733 about 0.80. This is a frequent example of EM algorithm finding local (instead of
734 global) maxima of the penalized log-likelihood. For such the case the likelihood of
735 the background model is higher, which implies that the found signal component is

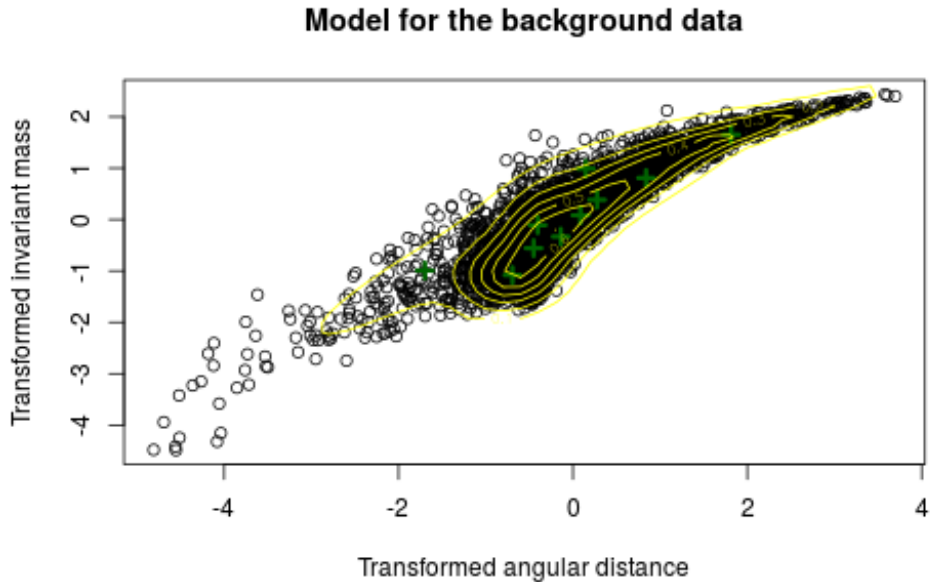


Figure 8: The plot of the two variables for the transformed background data to which the 10 component model was fitted. The green crosses are the component means and the contour reflects the estimated distribution of the sample.

736 spurious.

737 In order to find a non-spurious signal component, the algorithm should start
 738 with different initialization values as the EM algorithm is known to be sensitive to
 739 the starting point. The best practice is to use signal events for a starting value of sig-
 740 nal component mean. In this way it is more likely that a signal component is found
 741 and the global maximum is reached. However in general, it is not known which ob-
 742 servations are generated by the signal process and hence, the algorithm should be
 743 run multiple times starting from different initial values. The runs are performed as
 744 long as some fitted signal component increases the model likelihood with respect to
 745 the pure background model likelihood on the mixed data. In the following, we con-
 746 sider not only an increase of the likelihood but rather more conservative decrease
 747 of the modified BIC criteria.

748 The simulation results are presented in tables 3 and 4. The first one shows that
 749 the estimated fraction of the signal events is accurate, although a little biased to-
 750 ward the higher values. With decreasing true signal proportion λ the number of
 751 misclassified signal events rises 4. This affect the mean adjusted Rand index.

752 For signal proportions λ lower than 0.013, the algorithm has severe problems to
 753 fit a proper signal component. Note that already for $n = 4000$ and $\lambda = 0.013$ there
 754 are only 52 signal observations that the algorithm is sensitive to signal proportion
 755 $\lambda = 0.015$ is already satisfactory. However, it should be noted that distribution of

Table 3: Summary of the anomaly detection results performed by the PAD algorithm for datasets with different signal proportions λ . For each λ 50 datasets were generated in order to obtain also the standard deviations of the average estimates (in brackets).

| True signal proportion λ | Average estimate $\hat{\lambda}$ | Average adj. Rand index |
|----------------------------------|----------------------------------|-------------------------|
| 0.050 | 0.05099 (0.00021) | 0.9526 (0.0015) |
| 0.030 | 0.03093 (0.00025) | 0.9364 (0.0022) |
| 0.020 | 0.02129 (0.00043) | 0.9203 (0.0044) |
| 0.015 | 0.01658 (0.00033) | 0.8997 (0.0062) |

Table 4: Average percent of misclassification errors for the anomaly detection results performed by the PAD algorithm for the datasets with different signal proportions λ for the mixed data. For varying parameter λ , 50 datasets were generated in order to obtain the average estimates and their standard deviations (in brackets).

| Signal prop. λ | Average percent of misclassified signal observations | Average percent of misclassified background observations |
|------------------------|--|--|
| 0.050 | 2.39 (0.31) | 0.38 (0.11) |
| 0.030 | 3.87 (0.41) | 0.24 (0.07) |
| 0.020 | 6.66 (0.94) | 0.17 (0.05) |
| 0.015 | 10.70 (0.99) | 0.14 (0.05) |

756 the simulated signal is quite different from the background distribution, that causes
 757 the anomaly detection problem to be trivial.

758 6 Conclusions

759 We have presented a novel method for collective anomaly detection that makes use
 760 of a semi-supervised approach and is able to jointly perform variable selection and
 761 parameter estimation (referred as PAD). Motivations for the algorithm development
 762 derive from the needs of New Physics model-independent searches at the LHC. PAD
 763 algorithm makes use of Gaussian mixture models as the mean for data density es-
 764 timation and further classification of anomalous observations. It extends the idea
 765 of fixed-background model that has been previously applied in the same context.
 766 The main contribution with respect to the mentioned model is to perform proper
 767 feature selection so that variables that exhibit signal deviation are not removed.
 768 Dimensionality reduction is performed based on the penalized approach stemmed
 769 from the unsupervised penalized model-based clustering methods.

770 As a proof of concept, we have tested the PAD algorithm in two scenarios: one

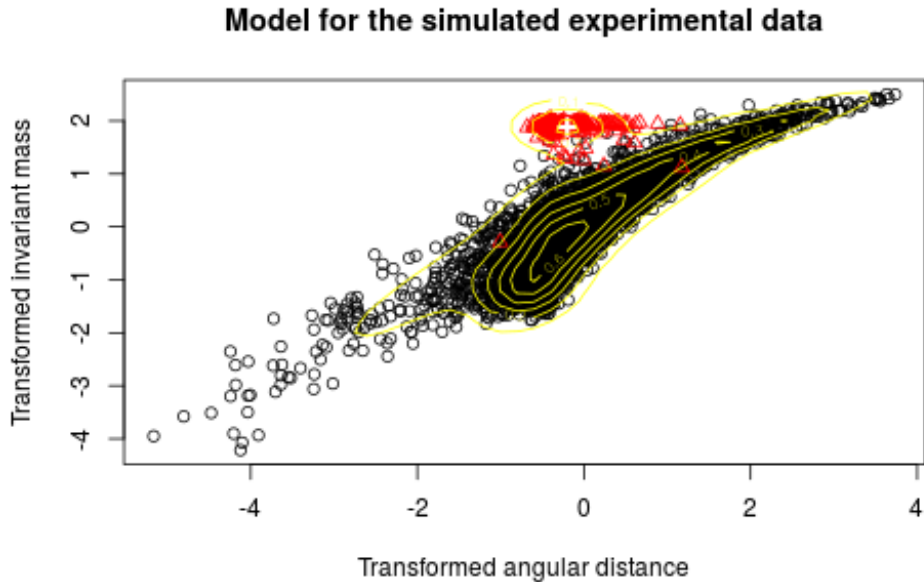


Figure 9: The plot of angular distance and invariant mass for the transformed simulated experimental data. Red dots and red triangles are respectively background and signal observations. The white cross is the signal component mean and the contour reflects the estimated distribution of the whole sample.

771 using idealized synthetic data and another one using data produced from MC simu-
 772 lators of high-energy collisions at the LHC, reconstructed as real data by the ATLAS
 773 detector. In the former case, the developed unsupervised model-based clustering
 774 method (called MAES) was tested. As well respective anomaly detection algorithm
 775 (PAD) was tested against different goals. The performance of both PAD and MAES
 776 was tested against other competing models with good results. The introduced di-
 777 mensionality technique turned out to be successful in removing uninformative vari-
 778 ables. The removal leads to better predictions. In the latter case, the method was
 779 used to detect an anomalous set of signal events coming from a simulated new
 780 physics process that yields two jets in the final state. The PAD algorithm enables
 781 to detect presence of an anomalous process, precisely estimate its proportion and
 782 estimate signal distribution.

783 **7 Acknowledgement**

784 The authors are grateful to the European Union's Horizon 2020 research and inno-
 785 vation program under grant agreement number 675440 for financial support.

786 8 Appendix

787 8.1 Pseudo-code for MAES algorithm

788 Function input:

- 789 • Background data - x
- 790 • Number of fitted components - K
- 791 • Maximal number of iteration allowed - n_iter
- 792 • Regularization parameters - γ_1 and γ_2
- 793 • Warm start initialization values for μ_k , π_k , Q_k and D_k for $k = 1; \dots, K$ (the de-
794 fault is NA)
- 795 • Stopping parameter ν

796 Algorithm

- 797 1. $P =$ dimension of x
- 798 2. $n =$ size of x
- 799 3. IF (any of $\pi_k^{(0)}$, $\mu_k^{(0)}$, $Q_k^{(0)}$ or $D_k^{(0)}$ for $k = 1, \dots, K$ is NA)
800 Initialize $\pi_k^{(0)} = \frac{1}{K}$, $Q_k^{(0)} = I_P$, $D_k^{(0)} = I_P$ and let $\mu_k^{(0)}$ be the centers of k-mean
801 algorithm
802 ELSE Check if initialization parameters are of right dimension, $\sum_{k=1}^K \pi_k = 1$
- 803 4. LikeLast = $-\infty$
- 804 5. LikeNew = the likelihood for the 0^{th} step
- 805 6. Iterator $r = 0$
- 806 7. While(|LikeLast-LikeNew| $> \nu$ AND $r < n_iter$)
 - 807 (a) Covariance matrices
808 For (k in 1:K)
$$\hat{\Sigma}_k^{(r)} = \hat{Q}_k^{(r)} \hat{D}_k^{(r)} \left(\hat{Q}_k^{(r)} \right)'. \quad (22)$$
 - 809 (b) Posterior probability
810 For (i in 1:n, l in 1:K)

$$\tau_{il}^{(r)} = \frac{\pi_l^{(r)} \phi\left(\mathbf{x}_i; \hat{\boldsymbol{\mu}}_l^{(r)}, \hat{\Sigma}_l^{(r)}\right)}{\sum_{k=1}^K \pi_k^{(r)} \phi\left(\mathbf{x}_i; \hat{\boldsymbol{\mu}}_k^{(r)}, \hat{\Sigma}_k^{(r)}\right)} \quad (23)$$

811 (c) Components proportions
812 For (k in 1:K)

$$\hat{\tau}_k^{(r+1)} = \frac{1}{n} \sum_{i=1}^n \tau_{ik}^{(r)}. \quad (24)$$

813 (d) MLE estimates
814 For (k in 1:K)

$$\tilde{\mu}_{kp}^{(r+1)} = \frac{\sum_{i=1}^n \tau_{ik}^{(r)} x_{ip}}{\sum_{i=1}^n \tau_{ik}^{(r)}} \quad (25)$$

815

$$\tilde{\Sigma}_k^{(r+1)} = \frac{\sum_{i=1}^n \tau_{ik}^{(r)} * (\mathbf{x}_i - \hat{\boldsymbol{\mu}}_k^{(r)})(\mathbf{x}_i - \hat{\boldsymbol{\mu}}_k^{(r)})'}{\sum_{i=1}^n \tau_{ik}^{(r)}} \quad (26)$$

(e) For (p in 1:P)

$$M_p^{(r)} = \max_{k=1, \dots, K} \hat{\Sigma}_{k,pp}^{(r)}$$

816 (f) For (k in 1:K) perform eigenvalue decomposition

$$\tilde{\Sigma}_k^{(r+1)} = \hat{Q}_k^{(r+1)} \tilde{D}_k^{(r+1)} \left(\hat{Q}_k^{(r+1)} \right)' \quad (27)$$

817 (g) FOR (k in 1:K, p in 1:P)

- IF $\left(\sum_{k=1}^K \left(\sum_{i=1}^n \tau_{ik}^{(r)} x_{ip} \right)^2 \right)^{\frac{1}{2}} \leq \gamma_1 M_p^{(r)}$

$$\hat{\mu}_{kp}^{(r+1)} = 0$$

- ELSE

$$\hat{\mu}_{kp}^{(r+1)} = \tilde{\mu}_{kp}^{(r+1)} - \gamma_1 \frac{\hat{\mu}_{kp}^{(r)} \Sigma_{k,pp}^{(r)}}{\|\hat{\boldsymbol{\mu}}_{\cdot p}^{(r)}\| \sum_{i=1}^n \tau_{ik}^{(r)}}$$

818 (h) FOR (k in 1:K)

-

$$\bar{D}_{k,pp}^{(r+1)} = \frac{-n\hat{\tau}_k^{(r+1)} + \sqrt{\left(n\hat{\tau}_k^{(r+1)} \right)^2 + 8\gamma_2 n\hat{\tau}_k^{(r+1)} \tilde{D}_{k,pp}^{(r)}}}{4\gamma_2}. \quad (28)$$

819 • To surpass numerical instability it is used
820 For (p in 1:P)

821 IF $\bar{D}_{k,pp}^{(r+1)} < 0.0005$ then $\bar{D}_{k,pp}^{(r+1)} = 0.0005$.

822 (i) FOR (k in 1:K, p in 1:P)

- 823 i. $\epsilon_k = \text{mean}(P - p + 1 \text{ smallest eigenvalues of } \bar{D}_k^{(r+1)})$.
 824 ii. For arbitrarily $\alpha = 0.05$

$$\text{Logical} = \frac{\bar{D}_{k,pp}^{(r+1)}}{\epsilon_k} < 1 - \sqrt{\frac{2}{n}} * z_{\frac{\alpha}{2p}} \vee \frac{\bar{D}_{k,pp}^{(r+1)}}{\epsilon_k} > 1 + \sqrt{\frac{2}{n}} * z_{\frac{\alpha}{2p}}$$

824 where $z_{\frac{\alpha}{2p}}$ is a normal distribution quantile.

- 825 iii. If ($\text{Logical} = \text{true}$) then the smallest $P - p + 1$ eigenvalues $\hat{D}_{k,pp}^{(r+1)} =$
 826 $\dots = \hat{D}_{k,pp}^{(r+1)} = \epsilon_k$
 827 BREAK the inner loop over 1:P.

- 828 iv. else $\hat{D}_{k,pp}^{(r+1)} = \bar{D}_{k,pp}^{(r+1)}$.

829 (j) LikeLast = LikeNew

830 (k) LikeNew = likelihood for the $(r + 1)^{th}$ step.

- 831 8. Return all the parameters value for the last step and an error code if n_iter was
 832 reached (issues with convergence in n_iter steps)

The algorithm should be run for different values of γ_1 , γ_2 and K to perform the optimal selection, that is the one that minimizes the modified BIC criteria

$$-2\log L(\hat{\Theta}) + \log(n)d_{eff}$$

833 where d_{eff} is effective number of degrees of freedom.

834 8.2 Pseudo-code for anomaly detection PAD algorithm

835 Function of:

- 836 • Mixed data - γ
- 837 • Number of signal components - L
- 838 • Maximal number of iteration allowed - n_iter
- 839 • Regularization parameters - γ_1 and γ_2
- 840 • Warm start initialization values for λ , μ_k , π_k , Q_k and D_k for $k = 1; \dots, K + L$ (the
 841 default is NA)
- 842 • Stopping parameter ν

843 Algorithm

- 844 1. $P = \text{dimension of } \gamma$

- 845 2. $n = \text{size of } y$
- 846 3. IF (any of $\pi_k^{(0)}$, $\mu_k^{(0)}$, $Q_k^{(0)}$ or $D_k^{(0)}$ for $k = K + 1, \dots, K + L$ is NA)
- 847 Initialize $\pi_k^{(0)} = \frac{1}{L} * \lambda$, $Q_k^{(0)} = I_p$, $D_k^{(0)} = I_p$ and let $\mu_k^{(0)}$ be random
- 848 ELSE Check if initialization parameters are of right dimension, $\sum_{k=1}^K \pi_k = 1$
- 849 4. For (k in 1:K) $\pi_k^{(0)} = (1 - \lambda)\pi_k^{(0)}$
- 850 5. LikeLast = $-\infty$
- 851 6. LikeNew = the likelihood for the 0^{th} step computed based on y
- 852 7. Iterator $r = 0$
- 853 8. While(|LikeLast-LikeNew| > ν AND $r < n_iter$)

- 854 (a) Covariance matrices
- 855 For (k in K+1:K+L)

$$\hat{\Sigma}_k^{(r)} = \hat{Q}_k^{(r)} \hat{D}_k^{(r)} \left(\hat{Q}_k^{(r)} \right)' \quad (29)$$

- 856 (b) Posterior probability
- 857 For (i in 1:n, l in 1:K+L)

$$\tau_{il}^{(r)} = \frac{\pi_l^{(r)} \phi\left(\mathbf{x}_i; \hat{\boldsymbol{\mu}}_l^{(r)}, \hat{\Sigma}_l^{(r)}\right)}{\sum_{k=1}^K \pi_k^{(r)} \phi\left(\mathbf{x}_i; \hat{\boldsymbol{\mu}}_k^{(r)}, \hat{\Sigma}_k^{(r)}\right)} \quad (30)$$

- 858 (c) Components proportions
- 859 For (k in K+1:K+L)

$$\hat{\pi}_k^{(r+1)} = \frac{1}{n} \sum_{i=1}^n \tau_{ik}^{(r)} \quad (31)$$

- 860 (d) $\hat{\lambda}^{(r+1)} = \sum_{k=K+1}^{K+L} \hat{\pi}_k^{(r+1)}$

- (e) Reweighing of the background proportions
- For (k in 1:K)

$$\hat{\pi}_k^{(r+1)} = \hat{\pi}_k^{(r)} * (1 - \lambda^{(r+1)}) / \left(\sum_{k=1}^K \hat{\pi}_k^{(r)} \right)$$

- 861 (f) MLE estimates
- 862 For (k in K+1:K+L)

$$\tilde{\boldsymbol{\mu}}_{kp}^{(r+1)} = \frac{\sum_{i=1}^n \tau_{ik}^{(r)} x_{ip}}{\sum_{i=1}^n \tau_{ik}^{(r)}} \quad (32)$$

863

$$\tilde{\Sigma}_k^{(r+1)} = \frac{\sum_{i=1}^n \tau_{ik}^{(r)} * (\mathbf{x}_i - \hat{\boldsymbol{\mu}}_k^{(r)}) (\mathbf{x}_i - \hat{\boldsymbol{\mu}}_k^{(r)})'}{\sum_{i=1}^n \tau_{ik}^{(r)}} \quad (33)$$

(g) For (p in 1:P)

$$M_p^{(r)} = \max_{k=1, \dots, K+L} \hat{\Sigma}_{k,pp}^{(r)}$$

864

(h) For (k in K+1:K+L) perform eigenvalue decomposition

$$\tilde{\Sigma}_k^{(r+1)} = \hat{Q}_k^{(r+1)} \tilde{D}_k^{(r+1)} \left(\hat{Q}_k^{(r+1)} \right)' \quad (34)$$

865

(i) FOR (k in K+1:K+L, p in 1:P)

- IF $\left(\sum_{k=1}^K \left(\sum_{i=1}^n \tau_{ik}^{(r)} x_{ip} \right)^2 \right)^{\frac{1}{2}} \leq \gamma_1 M_p^{(r)}$

$$\hat{\boldsymbol{\mu}}_{kp}^{(r+1)} = 0$$

- ELSE

$$\hat{\boldsymbol{\mu}}_{kp}^{(r+1)} = \tilde{\boldsymbol{\mu}}_{kp}^{(r+1)} - \gamma_1 \frac{\hat{\boldsymbol{\mu}}_{kp}^{(r)} \Sigma_{k,pp}^{(r)}}{\|\hat{\boldsymbol{\mu}}_{kp}^{(r)}\| \sum_{i=1}^n \tau_{ik}^{(r)}}$$

866

where the L_2 norm is computed based on background and signal mean parameters.

867

868

(j) FOR (k in K+1:K+L)

•

$$\bar{D}_{k,pp}^{(r+1)} = \frac{-n\hat{\tau}_k^{(r+1)} + \sqrt{\left(n\hat{\tau}_k^{(r+1)} \right)^2 + 8\gamma_2 n\hat{\tau}_k^{(r+1)} \tilde{D}_{k,pp}^{(r)}}}{4\gamma_2} \quad (35)$$

869

- To achieve numerical stability

870

For (p in 1:P)

871

IF $\bar{D}_{k,pp}^{(r+1)} < 0.0005$ then $\bar{D}_{k,pp}^{(r+1)} = 0.0005$.

872

(k) FOR (k in K+1:K+L, p in 1:P)

873

i. $\epsilon_k = \text{mean} (P - p + 1 \text{ smallest eigenvalues of } \bar{D}_k^{(r+1)})$.ii. For $\alpha = 0.05$

$$\text{Logical} = \frac{\bar{D}_{k,pp}^{(r+1)}}{\epsilon_k} < 1 - \sqrt{\frac{2}{n}} * z_{\frac{\alpha}{2p}} \vee \frac{\bar{D}_{k,pp}^{(r+1)}}{\epsilon_k} > 1 + \sqrt{\frac{2}{n}} * z_{\frac{\alpha}{2p}}$$

874

where $z_{\frac{\alpha}{2p}}$ is the normal distribution quantile.

875 iii. If (*Logical = true*) then the smallest $P - p + 1$ eigenvalues $\hat{D}_{k,pp}^{(r+1)} =$
876 ... = $\hat{D}_{k,pp}^{(r+1)} = \epsilon_k$
877 BREAK the inner loop over 1:P.
878 iv. else $\hat{D}_{k,pp}^{(r+1)} = \bar{D}_{k,pp}^{(r+1)}$.

879 (l) Perform the "Background fit" on x with slightly changed formulas

- in 7e

$$M_p^{(r)} = \max_{k=1, \dots, K+L} \hat{\Sigma}_{k,pp}^{(r)}$$

- in 7g mind the signal components

$$\|\hat{\mu}_{.p}^{(r)}\| = \sqrt{\sum_{k=1}^{K+L} \hat{\mu}_{kp}^{(r)2}}$$

insted of used previously

$$\|\hat{\mu}_{.p}^{(r)}\| = \sqrt{\sum_{k=1}^K \hat{\mu}_{kp}^{(r)2}}$$

880 (m) LikeLast = LikeNew

881 (n) LikeNew = likelihood for the $(r + 1)^{th}$ step.

882 9. Return all the parameters value for the last step and an error code if n_iter was
883 reached (issues with convergence in n_iter steps)

884 References

- 885 [1] S. Caron, A General Search for New Phenomena (2004). Talk given at HERA-
886 LHC Workshop (2004), available at [http://www.nikhef.nl/~scaron/talks/](http://www.nikhef.nl/~scaron/talks/heralhctalk.pdf)
887 [heralhctalk.pdf](http://www.nikhef.nl/~scaron/talks/heralhctalk.pdf).
- 888 [2] N. Craig, P. Draper, K. Kong, Y. Ng, D. Whiteson, The unexplored landscape
889 of two-body resonances, arXiv 1610.09392 (2016).
- 890 [3] J. Alwall, R. Frederix, S. Frixione, V. Hirschi, F. Maltoni, O. Mattelaer, H. S.
891 Shao, T. Stelzer, P. Torrielli, M. Zaro, The automated computation of tree-
892 level and next-to-leading order differential cross sections, and their matching
893 to parton shower simulations, JHEP 07 (2014) 079.
- 894 [4] T. Sjostrand, S. Mrenna, P. Z. Skands, PYTHIA 6.4 Physics and Manual, JHEP
895 05 (2006) 026.
- 896 [5] T. Sjöstrand, S. Ask, J. R. Christiansen, R. Corke, N. Desai, P. Ilten, S. Mrenna,
897 S. Prestel, C. O. Rasmussen, P. Z. Skands, An Introduction to PYTHIA 8.2,
898 Computer Physics Communications 191 (2015) 159–177.
- 899 [6] J. de Favereau, C. Delaere, P. Demin, A. Giammanco, V. Lemaître, A. Mertens,
900 M. Selvaggi, DELPHES 3, A modular framework for fast simulation of a generic
901 collider experiment, JHEP 02 (2014) 057.
- 902 [7] ATLAS Collaboration, Search for high-mass dilepton resonances in pp colli-
903 sions at $\sqrt{s} = 8$ tev with the atlas detector, Physical Review D-Particles, Fields,
904 Gravitation and Cosmology 90 (2014).
- 905 [8] CMS Collaboration, Search for lepton flavour violating decays of heavy reso-
906 nances and quantum black holes to an $e\mu$ pair in proton-proton collisions at
907 $\sqrt{s} = 8$ TeV, The European Physical Journal C76 (2016) 317.
- 908 [9] CMS Collaboration, Model Unspecific Search for New Physics in pp Collisions
909 at $\sqrt{s} = 7$ TeV (2011).
- 910 [10] CMS Collaboration, MUSiC, a Model Unspecific Search for New Physics, in pp
911 Collisions at $\sqrt{s} = 8$ TeV (2017).
- 912 [11] ATLAS Collaboration, A general search for new phenomena with the ATLAS
913 detector in pp collisions at $\sqrt{s} = 8$ TeV (2014).
- 914 [12] ATLAS Collaboration, A general search for new phenomena with the ATLAS
915 detector in pp collisions at $\sqrt{s} = 7$ TeV. (2012).
- 916 [13] ATLAS Collaboration, A model independent general search for new phenom-
917 ena with the ATLAS detector at $\sqrt{s} = 13$ TeV (2017).

- 918 [14] V. Chandola, A. Banerjee, V. Kumar, Anomaly detection: A survey, Association
919 for Computing Machinery computing surveys (CSUR) 41 (2009) 15.
- 920 [15] T. Vatanen, M. Kuusela, E. Malmi, T. Raiko, T. Aaltonen, Y. Nagai, Semi-
921 supervised detection of collective anomalies with an application in high energy
922 particle physics, The 2012 International Joint Conference on Neural Networks
923 (2012) 1–8.
- 924 [16] M. Kuusela, T. Vatanen, E. Malmi, T. Raiko, T. Aaltonen, Y. Nagai, Semi-
925 supervised anomaly detection – towards model-independent searches of new
926 physics, Journal of Physics: Conference Series 368 (2012) 012032.
- 927 [17] C. Fraley, A. E. Raftery, Model-based clustering, discriminant analysis, and
928 density estimation, Journal of the American statistical Association 97 (2002)
929 611–631.
- 930 [18] A. P. Dempster, N. M. Laird, D. B. Rubin, Maximum likelihood from incom-
931 plete data via the em algorithm, Journal of the royal statistical society. Series
932 B (methodological) (1977) 1–38.
- 933 [19] R. Alexandridis, S. Lin, M. Irwin, Class discovery and classification of tumor
934 samples using mixture modeling of gene expression data - a unified approach,
935 Bioinformatics 20 (2004) 2545–2552.
- 936 [20] J. D. Banfield, A. E. Raftery, Model-based gaussian and non-gaussian cluster-
937 ing, Biometrics (1993) 803–821.
- 938 [21] G. Celeux, G. Govaert, Gaussian parsimonious clustering models, Pattern
939 recognition 28 (1995) 781–793.
- 940 [22] C. Bouveyron, S. Girard, C. Schmid, High-dimensional data clustering, Com-
941 putational Statistics & Data Analysis 52 (2007) 502–519.
- 942 [23] A. E. Hoerl, R. W. Kennard, Ridge regression: Biased estimation for nonorthog-
943 onal problems, Technometrics 12 (1970) 55–67.
- 944 [24] B. Efron, T. Hastie, I. Johnstone, R. Tibshirani, et al., Least angle regression,
945 The Annals of statistics 32 (2004) 407–499.
- 946 [25] R. Tibshirani, Regression shrinkage and selection via the lasso, Journal of the
947 Royal Statistical Society. Series B (Methodological) (1996) 267–288.
- 948 [26] W. Pan, X. Shen, Penalized model-based clustering with application to variable
949 selection, Journal of Machine Learning Research 8 (2007) 1145–1164.
- 950 [27] B. Xie, Variable selection in penalized model-based clustering, University of
951 Minnesota (2008).

- 952 [28] H. Zhou, W. Pan, X. Shen, Penalized model-based clustering with uncon-
953 strained covariance matrices, *Electronic journal of statistics* 3 (2009) 1473.
- 954 [29] B. Xie, W. Pan, X. Shen, Variable selection in penalized model-based clustering
955 via regularization on grouped parameters, *Biometrics* 64 (2008) 921–930.
- 956 [30] M. Yuan, Y. Lin, Model selection and estimation in regression with grouped
957 variables, *Journal of the Royal Statistical Society: Series B (Statistical Method-*
958 *ology)* 68 (2006) 49–67.
- 959 [31] W. Pan, X. Shen, A. Jiang, R. P. Hebbel, Semi-supervised learning via penalized
960 mixture model with application to microarray sample classification, *Bioinfor-*
961 *matics* 22 (2006) 2388–2395.
- 962 [32] P. Bühlmann, S. Van De Geer, *Statistics for high-dimensional data: methods,*
963 *theory and applications*, Springer Science & Business Media (2011) 298–300.
- 964 [33] M. L. Eaton, *Multivariate statistics: A vector space approach*, Beachwood,
965 Ohio, USA: Institute of Mathematical Statistics (2007).
- 966 [34] C. E. Bonferroni, *Teoria statistica delle classi e calcolo delle probabilita*, Libreria
967 internazionale Seeber (1936).
- 968 [35] G. Schwarz, Estimating the dimensions of a model, *Annals of Statistics* (1978)
969 461–464.
- 970 [36] R Core Team, *R: A language and environment for statistical computing*, R
971 Foundation for Statistical Computing, <https://www.R-project.org/> (2017).
- 972 [37] L. Scrucca, M. Fop, T. B. Murphy, A. E. Raftery, mclust 5: clustering, classi-
973 fication and density estimation using Gaussian finite mixture models, *The R*
974 *Journal* 8 (2016) 205–233.
- 975 [38] L. Bergé, C. Bouveyron, S. Girard, HDclassif: An R package for model-based
976 clustering and discriminant analysis of high-dimensional data, *Journal of Sta-*
977 *tistical Software* 46 (2012) 1–29.
- 978 [39] J. M. Santos, M. Embrechts, On the use of the adjusted rand index as a metric
979 for evaluating supervised classification (2009) 175–184.
- 980 [40] W. M. Rand, Objective criteria for the evaluation of clustering methods, *Jour-*
981 *nal of the American Statistical association* 66 (1971) 846–850.
- 982 [41] B. Fuks, Beyond the Minimal Supersymmetric Standard Model: from theory to
983 phenomenology, *International Journal of Modern Physics A* 27 (2012) 1230007.
- 984 [42] R. Barbier, et al., R-parity violating supersymmetry, *Physical Review* 420
985 (2005) 1–202.

- 986 [43] The minimal supersymmetric standard model with r-parity violation (2012).
- 987 [44] R. D. Ball, et al., Parton distributions with LHC data, Nuclear Physics B867
988 (2013) 244–289.
- 989 [45] C. Chen, New approach to identifying boosted hadronically-decaying particle
990 using jet substructure in its center-of-mass frame, Physical Review D85 (2012)
991 034007.
- 992 [46] J. W. Tukey, Exploratory data analysis, Reading: Addison-Wesley (1977).
- 993 [47] Z. S. Abdallah, L. Du, G. I. Webb, Data preparation, Encyclopedia of Machine
994 Learning and Data Mining (2016) 1–11.